Development/Plasticity/Repair

Induction of Vertebrate Regeneration by a Transient Sodium Current

Ai-Sun Tseng,[1,2,3,4] **Wendy S. Beane,**[1,2] **Joan M. Lemire,**[1,2] **Alessio Masi,**[1,2] **and Michael Levin**[1,2,3,4]

[1]Department of Biology and [2]Center for Regenerative and Developmental Biology, Tufts University, Medford, Massachusetts 02155, and [3]Forsyth Institute and [4]Harvard School of Dental Medicine, Boston, Massachusetts 02155

Amphibians such as frogs can restore lost organs during development, including the lens and tail. To design biomedical therapies for organ repair, it is necessary to develop a detailed understanding of natural regeneration. Recently, ion transport has been implicated as a functional regulator of regeneration. Whereas voltage-gated sodium channels play a well known and important role in propagating action potentials in excitable cells, we have identified a novel role in regeneration for the ion transport function mediated by the voltage-gated sodium channel, $Na_V1.2$. A local, early increase in intracellular sodium is required for initiating regeneration following *Xenopus laevis* tail amputation, and molecular and pharmacological inhibition of sodium transport causes regenerative failure. $Na_V1.2$ is absent under nonregenerative conditions, but misexpression of human $Na_V1.5$ can rescue regeneration during these states. Remarkably, pharmacological induction of a transient sodium current is capable of restoring regeneration even after the formation of a nonregenerative wound epithelium, confirming that it is the regulation of sodium transport that is critical for regeneration. Our studies reveal a previously undetected competency window in which cells retain their intrinsic regenerative program, identify a novel endogenous role for Na_V in regeneration, and show that modulation of sodium transport represents an exciting new approach to organ repair.

Introduction

Humans have limited ability to repair injured or damaged organs. Interestingly, most mammalian organs contain resident progenitor cells (Zupanc, 2006), but it is not known why these cells are not mobilized for repair, suggesting that there may be an absence of instructive signals. Recently, it has become clear that biophysical signals such as ion currents and patterned voltage gradients (Reid et al., 2005; Adams et al., 2007) are key components for the induction of regeneration and patterning of new tissue in structures such as amphibian limbs and mammalian corneas (Zhao et al., 2006; Adams et al., 2007). To identify the molecular basis for regenerative currents in regeneration, we used *Xenopus laevis*—a powerful model that fully restores its larval appendages upon injury, uses pathways conserved to mammalian regeneration, and regenerates, as do mammals, through tissue renewal and not transdifferentiation (Gargioli and Slack, 2004; Slack et al., 2004; Chen et al., 2006).

The *Xenopus* larval tail is a complex organ containing multiple cell types: muscle, peripheral nerves, spinal cord, notochord, skin, and vasculature. After tail amputation, wound healing occurs within 6–8 h postamputation (hpa). By 24 hpa, an initial swelling containing progenitor cells, called the regeneration bud, is formed at the injury site. Subsequently, tissue outgrowth and patterning begin as the tail is rebuilt over ~7 d (Beck et al., 2009).

Several molecular components regulating tail regeneration have been identified. TGF-β signaling is required for proper wound healing and is detected at the wound as early as 15 min after amputation (Ho and Whitman, 2008). The proton (H^+) pump, V-ATPase, is active by 6 h postamputation, and its modulation of the transmembrane potential in regeneration bud cells is required during the first 24 hpa (Adams et al., 2007). Apoptosis in the regeneration bud during the first 24 hpa is also required for regeneration as in other systems (Tseng et al., 2007; Chera et al., 2009; Li et al., 2010). Components of signaling pathways such as BMP, Notch, Wnt, and FGF are expressed later and are involved in driving regenerative outgrowth and patterning (Beck et al., 2006; Mochii et al., 2007), recapitulating their well characterized roles during axial development. Several of these pathways have been targeted to induce regeneration of spinal cord and other tissues in nonregenerative states. To date, all of these functional interventions were applied before the actual injury. However, in order for significant advances in regenerative biomedicine to occur, it is necessary to identify new pathways that can be targeted by therapies to induce appendage regeneration after injury and nonpermissive wound healing.

Received June 26, 2010; revised Aug. 5, 2010; accepted Aug. 11, 2010.

This work was supported by the National Institutes of Health (Grant R01-GM078484 to M.L. and Grant F32-GM083547 to W.S.B.) and National Highway Traffic Safety Administration (Grant DTNH22-06-G-00001), Department of Defense (Grant W81XWH-10-2-0058), and Defense Advanced Research Projects Agency (Grant W911NF-07-1-0572) grants to M.L. We thank D. Adams for assistance with dye imaging and confocal microscopy, P. Koustubhan and A. Currier for their assistance with *Xenopus* husbandry, D. Qiu and J. Boltax for technical assistance and histology, and F. Miskevich for advice about generating RNAi targeting constructs. Clones for $XNa_V1.2$ and $XNa_V1.5$ were gifts from M. Kukuljan. Clone for $hNa_V1.5$ was a gift from M. Djamgoz. The cloning vector for RNAi was a gift from F. Miskevich. We are grateful for the advice and support of P. Smith at the BioCurrents Resource Center.

Correspondence should be addressed to Michael Levin, Center for Regenerative and Developmental Biology, Tufts University, Suite 4600, 200 Boston Avenue, Medford, MA 02155. E-mail: michael.levin@tufts.edu.

A. Masi's present address: Dipartimento di Farmacologia, Università degli Studi di Firenze, 50139 Firenze, Italy.

A.-S. Tseng, W. S. Beane, J. M. Lemire, and M. Levin's present address: Center for Regenerative and Developmental Biology, Tufts University, 200 Boston Avenue, Medford, MA 02155.

DOI:10.1523/JNEUROSCI.3315-10.2010

 0270-6474/10/3013192-09$15.00/0

Here we identify a new mechanism controlling vertebrate regeneration by modulating *in vivo* sodium (Na^+) transport, endogenously mediated by the voltage-gated sodium channel, $Na_V1.2$. Crucially, direct modulation of sodium transport is sufficient to induce vertebrate regeneration even after a nonregenerative wound epithelium has formed. Our data reveal a novel bioelectrical regulator of regeneration, and suggest a new therapeutic approach independent of transgenesis that can promote the regeneration of a complex appendage.

Materials and Methods

Tail regeneration assay. *Xenopus laevis* larvae were cultured via approved protocols (Institutional Animal Care and Use Committee, #M2008-08). Tails at stages (st.) 40–41 (regenerative) or 45–47 (refractory period) (Nieuwkoop and Faber, 1967) were amputated at the midpoint between the anus and the tip. Tadpoles were cultured in 0.1× MMR, with or without reagent, at 22°C for 7 d and scored for tail regeneration. Unless indicated, 250 μM MS222 (Sigma) was used for assays. To quantify and compare regeneration in groups of tadpoles treated with different reagents, we determined a composite regeneration index (RI), ranging from 0 (no regeneration) to 300 (complete regeneration) as described previously (Adams et al., 2007). This index, and the specific definitions of regeneration phenotype categories (full, good, weak, none) are given in supplemental Figure S1 (available at www.jneurosci.org as supplemental material). For example, a group of tails in which >80% were fully regenerated would have an RI ranging from 240 to 300; if full regeneration occurred in <10% of the animals within the group, the RI would range from 0 to 30.

RNA interference and embryo injections. DNA oligos encoding short hairpin RNAs (shRNA) targeting *Xenopus* $Na_V1.2$ (AY121368), dsRed (AY679106), or salt-inducible kinase (SIK; 1319975) were cloned downstream of a U6 RNA Pol III promoter; the vector also contained cytomegalovirus-driven green fluorescent protein (GFP) (Miskevich et al., 2006). RNA interference (RNAi) target sequences are as follows: $Na_V1.2$, 5′-GCCATGGAGCATTATCCAATG-3′; dsRed, 5′-GTTCAAGTCCATCTACATGGC-3′; and SIK, 5′-GCCAGTTCTCTACTCACAAAC-3′. These constructs were microinjected into one- or two-cell stage embryos. The presence of the shRNA in st. 40 tail tissues was identified by GFP fluorescence, indicating that the plasmid was expressed in the cells. For overexpression, full-length β-galactosidase or human $Na_V1.5$ (GI:184038) RNA were transcribed using mMessage Machine kit (Ambion). Approximately 5 ng of each target was mixed with 500 pg of GFP mRNA and was injected into two-cell embryos. Tails with good GFP expression were selected before amputation for experiments.

Modulation of sodium flux and imaging of reporter dyes. At 23 hpa, st. 40 tadpoles were incubated in 90 μM CoroNa Green indicator dye (Invitrogen) in 0.1× MMR for 45 min and washed twice in 0.1× MMR and 30 μM *N*-benzyl-p-toluene sulfonamide (BTS; Tocris Bioscience) to immobilize tadpole movement. At 24 hpa, the CoroNa Green signal was excited at 488 nm and fluorescence emission data were collected at 516 nm. Data were analyzed using IPLab software (BD Biosciences). For induction of Na^+ current, 0.1× MMR was supplemented with sodium gluconate (Sigma) to increase the Na^+ concentration to 90 mM. For refractory period analysis, tails were amputated at st. 46–47, and at 18 hpa animals were treated with or without 90 mM sodium and 20 μM monensin (Sigma) in 0.1× MMR with 90 μM CoroNa Green for 45 min and washed twice in 0.1× MMR and 50 μM BTS. Imaging of transmembrane potential using DiBAC4(3) (Invitrogen) with controls was performed exactly as described previously (Adams et al., 2007).

In situ *hybridization and immunohistochemistry.* *In situ* hybridization was performed according to standard protocols (Harland, 1991) with probes to $Na_V1.2$ (AY121368), $Na_V1.5$ (Armisén et al., 2002), Notch1 (Coffman et al., 1990), Msx1 (Feledy et al., 1999), and SIK (1319975). *Xenopus* embryos were fixed overnight in MEMFA buffer (Sive et al., 2000), heated for 2 h at 65°C in 50% formamide (to inactivate endogenous alkaline phosphatases), permeabilized in PBS and 0.1% Triton X-100 for 30 min, and processed for immunohistochemistry using alkaline phosphatase secondary antibody (Levin, 2004) until signal was optimal and background minimal. The expression profiles represent consensus patterns obtained from the analysis of 8–12 tails at each stage. Anti-$Na_V1.2$ (Millipore), anti-acetylated α-tubulin (Sigma), and anti-phospho-H3 (Millipore) antibodies were used at 1:1000. Quantification of phospho-H3-positive cells were performed as described previously (Adams et al., 2007).

Cloning and gene expression. A tBLASTn search using mammalian SIK sequences identified a homologous *Xenopus laevis* cDNA clone #6641975 (accession #BU915306) in the *Xenopus* Gene Collection library. This clone was purchased and the sequence of this clone was submitted to GenBank (accession #1319975). Fifteen to twenty regeneration buds (st. 40; 24 hpa) were collected and RNA isolated by Trizol (Invitrogen). A cDNA library was generated using the SMART cDNA synthesis kit (Clontech). Primers designed to the sequence 5′-TCCAGTCAGTTTCCGAGAAGGCAGACG-3′ (forward); 5′-GCACCAGGTTCTGCATCTGCTGGGAATG'-3′ (reverse) were used to identify the presence of the *Xenopus* homolog in the cDNA library. To detect gene expression by reverse transcription PCR, 15–20 regeneration buds from amputated tail were collected and RNA isolated by Trizol (Invitrogen). RNA was reverse transcribed using the Quantitect RT kit (Qiagen) to generate cDNA for real-time PCR analysis. Primers used were NaV1.2 (forward, 5′-GCAGCCACTGCTACCCCCAC-3′; reverse, 5′-GCACTGCCACCATTCCCGGT-3′) and EF1 (forward, 5′-CAGGCCAGATTGGTGCTGGATATGC-3′; reverse, 5′-GCTCTCCACGCACATTGGCTTTCCT-3′). Target expression was normalized to EF1 expression.

Statistical analysis. To compare tail regeneration experiments, raw data from scoring was used. Comparison of two treatments was analyzed with Mann–Whitney *U* test for ordinal data with tied ranks, using normal approximation for large sample sizes. Multiple treatments were compared using a Kruskal–Wallis test, with Dunn's Q corrected for tied ranks. All other experiments were analyzed using a Student's *t* test.

Results

Requirement for sodium transport in regeneration

We identified a requirement for sodium transport in the course of a chemical genetics screen for bioelectric regulators specifically controlling regeneration (Adams et al., 2007). MS222 (tricaine) is a well known inhibitor of all voltage-gated sodium channels (VGSCs or Na_Vs) (Hedrick and Winmill, 2003) that blocks inward sodium currents (Frazier and Narahashi, 1975). Treatment of animals with either 150 or 250 μM MS222 immediately after tail amputation for the duration of the 7 d assay significantly inhibited regenerative ability, as calculated using the composite RI (supplemental Fig. S1, available at www.jneurosci.org as supplemental material) (RI = 114, $n = 65$; and RI = 44, $n = 63$, respectively) in a dose-dependent manner when compared with control siblings (RI = 265, $n = 68$, $p < 0.01$) (Fig. 1*A*,*B*). MS222 treatment did not induce significant apoptosis in the bud and overall development of the animals (including growth of the primary tail) was normal, suggesting that this is a regeneration-specific effect. Importantly, the concentrations used were approximately tenfold lower than those commonly used to induce tadpole paralysis (mM range) and the phenotypes we describe occur in tadpoles with normal behavior and mobility. To demonstrate the effect of MS222-mediated Na_V inhibition on sodium transport, we visualized sodium flux using CoroNa Green (Fig. 1*C*), a fluorescent sodium-indicator dye that selectively interacts with sodium ions and exhibits an increase in fluorescent emission upon binding (Meier et al., 2006). In intact tails, few cells appear positive for the CoroNa Green signal relative to the majority of the tail population. At 24 hpa, a strong CoroNa Green signal is seen in the regeneration bud region but not in the rest of the tail and trunk, suggesting a significant increase in sodium transport into the cells of the bud during regeneration. When the amputated tails were treated with MS222, the CoroNa Green signal was abolished ($n =$ 8 per treatment, $p < 0.005$), confirming that inhibition of Na_V

abrogates sodium influx into the bud. Therefore, we conclude that modulation of Na_V-dependent sodium flux in bud cells is an important regulator of regeneration.

Na_Vs, the target of MS222 action, are plasma membrane proteins that regulate sodium influx into cells (Yu and Catterall, 2003). In *Xenopus*, $Na_V1.2$ and $Na_V1.5$ have been identified, and we examined their expression in the regeneration bud. $Na_V1.5$ was not expressed (supplemental Fig. S2, available at www.jneurosci.org as supplemental material). Consistent with a role for $Na_V1.2$ in the early processes of tail regeneration, $Na_V1.2$ RNA was expressed by 18 hpa in the mesenchymal cells of the regeneration bud and persisted as late as 2 d postamputation (Fig. 1*D*). $Na_V1.2$ protein was similarly expressed (supplemental Fig. S2, available at www.jneurosci.org as supplemental material).

To confirm the molecular basis for the regeneration-relevant sodium signaling in tail regeneration, we next ablated $Na_V1.2$ activity by RNAi using a plasmid encoding a short RNA hairpin construct specifically targeting the *Xenopus* $Na_V1.2$ gene. The targeting vector carries a GFP marker (Miskevich et al., 2006) on the same plasmid, enabling the accurate selection of animals that expressed the RNAi construct in the distal tail. Real-time PCR quantification of $Na_V1.2$ mRNA in the regeneration bud at 24 hpa revealed an overall decrease of 40% when compared with controls, showing the effectiveness of $Na_V1.2$ RNAi knockdown *in vivo*. Despite the necessarily mosaic uptake of $Na_V1.2$ RNAi construct, expression of the $Na_V1.2$ short RNAi hairpin in the tail region at the site of amputation was able to significantly inhibit tail regeneration (RI = 198, $n = 100$, $p < 0.01$) compared with control RNAi targeting dsRed, a fluorescent protein that is not endogenous to *Xenopus* (RI = 261, $n = 72$), confirming our pharmacological loss-of-function data (Fig. 1*E*). Although we cannot rule out additional contributions from as-yet-unidentified Na_V isoforms, these data demonstrate that $Na_V1.2$ is specifically required for tail regeneration, reveal an important component of endogenous regenerative response in *Xenopus*, and identify a new role for voltage-gated sodium channels.

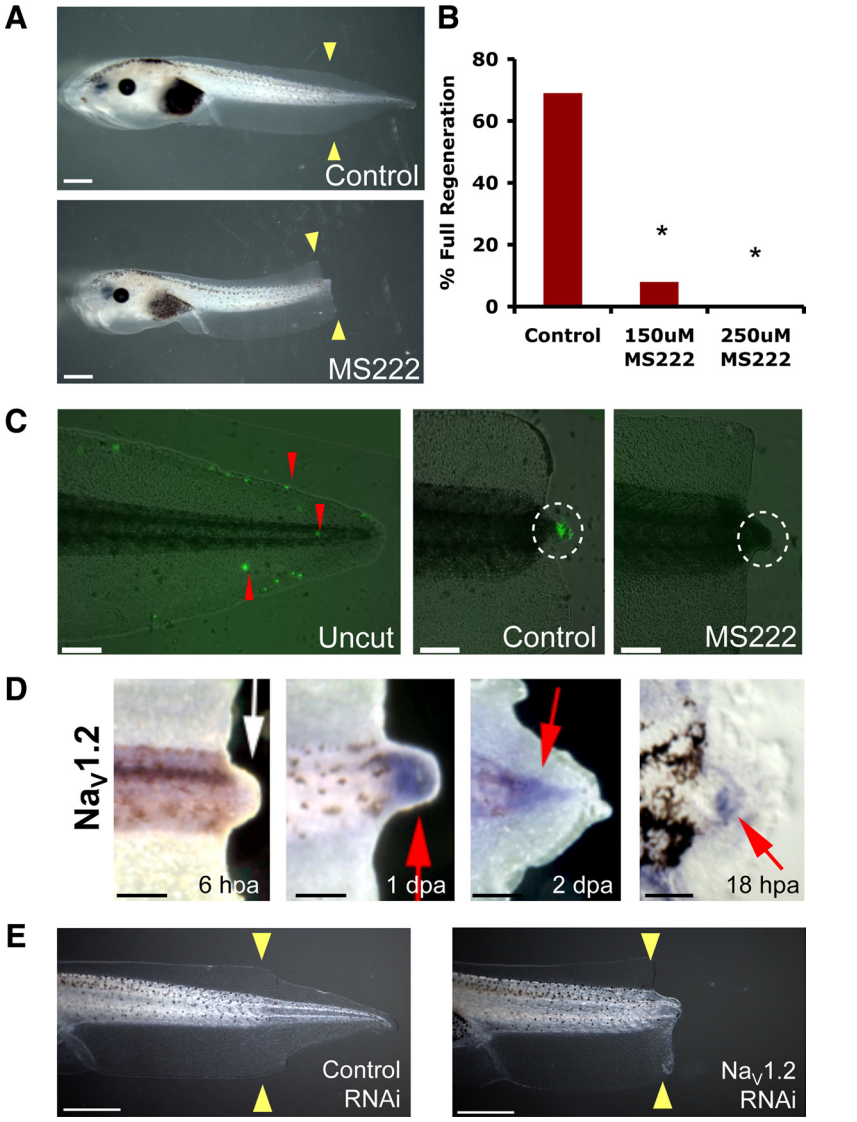

Figure 1. Sodium transport is required for tail regeneration. ***A***, Control tails amputated at st. 40 regenerate fully whereas siblings treated with 250 μM MS222 fail to regenerate. ***B***, Effects of Na_V chemical inhibition on regeneration showing dose-dependent inhibition. ***C***, Fluorescent indicator dye (CoroNa Green) of sodium flux (red arrows). Uncut tail has scattered fluorescence. Cut tail (24 hpa) shows strong sodium influx into the regeneration bud (white circle) in contrast to MS2222-treated buds. ***D***, Whole-mount *in situ* hybridization for $Na_V1.2$ in amputated tails. Regeneration bud (6 hpa) lacks $Na_V1.2$ expression. By 24 hpa, $Na_V1.2$ is expressed in the regeneration bud and persists until 48 hpa. A section through an 18 hpa regeneration bud reveals $Na_V1.2$ in mesenchymal cells but not the wound epidermis. ***E***, Control tails amputated at st. 40 regenerate fully but animals expressing Na_V RNAi construct do not. Scale bars: ***A***, ***E***, 1 mm; ***C***, ***D***, 500 μm; ***D***, far right, 100 μm. Red arrows, expression; white arrow, lack of expression; yellow arrows, amputation plane. dpa, Days postamputation. *$p < 0.001$.

Early control of regenerative processes by sodium influx

To examine the temporal requirement for Na_V-mediated sodium transport during regeneration, we amputated tails of tadpoles, treated them with 250 μM MS222 for specific durations, and assayed their regenerative ability. Exposure to Na_V blocker MS222 for the first 24 hpa prevented tail regeneration in 45% of the tadpoles ($n = 106$), indicating that sodium transport plays a role in regeneration bud establishment. When the duration of MS222 treatment was expanded to include the first 48 hpa, 78% of the tails failed to regenerate ($n = 105$), fully recapitulating the severity of phenotype seen when Na_V inhibition occured throughout the entire 7 d required for regeneration ($n = 103$). We then examined the effect of Na_V inhibition after amputation. MS222 treatment targeting Na_V activity at 24 hpa resulted in 26% regenerative failure ($n = 107$), demonstrating that the initial expression of $Na_V1.2$ at 18 hpa is critical to initiating regeneration. However, addition of MS222 at 48 hpa ($n = 63$), after regenerative outgrowth has begun, had no effect. Together, these results are consistent with our data for $Na_V1.2$ (Fig. 1*D*) and strongly suggest that sodium transport is principally required during the establishment and early outgrowth phases of regeneration. Given

this early role, we next asked what is the relationship between sodium influx and the known later steps in tail regenerative outgrowth?

Rapidly rebuilding a tail requires the increase of proliferating cells observed at the regeneration bud by 48 hpa (Adams et al., 2007). To understand the cellular basis for the regenerative failure caused by block of sodium transport, we examined proliferation in sodium flux-inhibited animals. During development, mitotic cells are observed to be randomly located in the growing tail (Adams et al., 2007). We quantified the number and distribution of proliferating cells in regenerating tails at 48 hpa using an antibody to phosphorylated histone 3B (H3P), a marker of the G_2/M transition of the cell cycle that identifies mitotic cells in *Xenopus* and many other systems (Saka and Smith, 2001; Adams et al., 2006). Na_V inhibition using MS222 treatment caused a 90% decrease in the number of mitotic cells in the regeneration bud region (1.3 ± 1.5, $n = 4$) compared with control siblings (12.5 ± 4.8, $n = 4$, $p < 0.005$). Many H3P-positive cells were seen in the wild-type regeneration bud but very few are detected in MS222-treated buds (Fig. 2*A*, top). Importantly, no significant change in proliferation was seen in the central tail flank region (71 ± 27 H3P-positive cells for controls compared with 66.3 ± 10 for MS222 treatment, $n = 8$, $p = 0.38$), showing that Na_V-mediated sodium flux is not a general requirement for normal cell division. Together, these data demonstrate that sodium transport is necessary for the specific upregulation of proliferation in the regenerative growth region.

Another important requirement for regenerative growth is proper innervation (Singer, 1952, 1965). Thus, we examined the neuronal pattern in the amputated tail stumps of tadpoles treated with MS222 (Fig. 2*A*, bottom). In normal, 3-d-old tail regenerates, axons appear in bundles that grow and concentrate toward the end of the regenerate, in a direction parallel to the anterior–posterior axis. In contrast, MS222 treatment caused axons to extend circumferentially along the edge of the regeneration bud, perpendicular to the main axis of tail growth. Notably, the overall quantity of neurons appeared to be reduced compared with control siblings. These results suggest that sodium flux is required for proper innervation of the regenerate.

Several pathways have been shown to be required for driving regenerative outgrowth and patterning in the tail, including Notch, Msx1, and BMP (Beck et al., 2003, 2006; Sugiura et al., 2004). To determine whether these pathways are controlled by sodium influx, we performed *in situ* hybridization using gene-specific RNA probes to examine the expression patterns of Notch and Msx1 in the regeneration bud after Na_V inhibition (Fig. 2*B*). At 48 hpa, Notch1 is normally expressed in the neural ampulla and in the mesenchymal region of the regeneration bud, and Msx1 is expressed in the neural ampulla and at the epithelial edge of the regenerating tail tip. In contrast, MS222 treatment largely abolished expression of Notch1 and Msx1. Likewise, levels of BMP2, BMP4, and Delta were greatly reduced in the presence of MS222 (supplemental Fig. S2, available at www.jneurosci.org as supplemental material). Although not evidence for direct regulation, these results demonstrate that sodium flux acts upstream to induce the later expression of several key genes known to control downstream regenerative outgrowth and patterning.

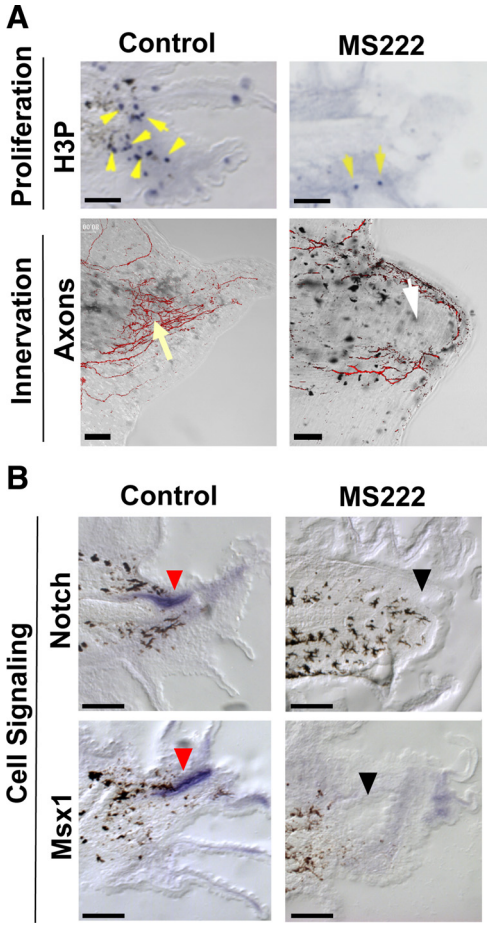

Figure 2. Na_V-mediated sodium transport acts early during regeneration. ***A***, Effect of Na_V inhibition (MS222) on proliferation and innervation. Top, Immunohistochemistry of 48 hpa tails using an anti-H3P antibody (blue) in sagittal sections (yellow arrows indicate mitotic cells; melanocytes are black). Bottom, Tails (72 hpa) stained with acetylated α-tubulin antibody to identify axons. Control axon bundles run parallel to the anterior–posterior axis and concentrate at the tip (yellow arrow). MS222 treatment reduces axons (white arrow) that trace along the edge. ***B***, Effect of Na_V inhibition on genes that regulate regenerative outgrowth (as shown by RNA *in situ* hybridization in sagittal sections at 48 hpa). Notch RNA (top) is expressed in the neural ampulla (red arrows) and in the regeneration bud mesenchyme, whereas Msx1 (bottom) is expressed solely in the neural ampulla. Gene expression is abolished after $Na_V1.2$ inhibition (black arrows). Scale bars, 250 μm.

Induction of regeneration by a transient sodium current

Mammals exhibit an age-dependent decrease in regenerative potential (Illingworth, 1974). Similarly, *Xenopus* tadpoles also show a loss of regenerative potential during the refractory period, an endogenous period (st. 45–47) during development in which tadpoles are unable to regenerate tails (Beck et al., 2003). Our results are consistent with $Na_V1.2$ expression being predictive of regenerative competency; it is absent in nonregenerating tail stumps, including those amputated during the refractory period (supplemental Fig. S2, available at www.jneurosci.org as supplemental material). Thus, induction of sodium current could be sufficient to promote regeneration during the nonregenerative refractory state.

Crucially, a primary role for sodium influx in the induction of reparative growth suggests that any functional Na_V could fulfill this requirement. We therefore expressed the human cardiac sodium channel, $Na_V1.5$ (Fraser et al., 2005), ubiquitously by early embryo injection and assessed its ability to rescue regeneration. As expected, ectopic expression of $hNa_V1.5$ in refractory cut tails, where endogenous $Na_V1.2$ is absent (supplemental Fig. S2, available at www.jneurosci.org as supplemental material), did indeed rescue regeneration (β-gal control, RI = 10, $n = 82$; compared with $hNa_V1.5$, RI = 39, $n = 116$, $p < 0.001$) (Fig. 3*A*,*B*). Support-

ing this observation, expression of $hNa_V1.5$ was also able to rescue regenerative failure (Adams et al., 2007) due to V-ATPase inhibition by concanamycin (β-gal control, RI = 120, $n = 145$; compared with $hNa_V1.5$, RI = 231, $n = 132$, $p < 0.0001$). These results confirm that sodium conductance, not a specific native Na_V protein, is required for driving regenerative outgrowth.

We next asked whether directly modulating sodium transport without genetic manipulation promotes regeneration. Monensin is an ionophore that selectively transports sodium ions into cells (Mollenhauer et al., 1990). Tails of animals in the refractory period were amputated and, at 18 hpa (recapitulating the timing of $Na_V1.2$ expression), treated with 20 μM monensin in a medium containing 90 mM sodium (normal culture medium contains 10 mM sodium). To confirm that monensin induces an increase in intracellular sodium levels, we used the CoroNa Green indicator dye to visualize sodium content in the amputated caudal stump. At 19 hpa, normal refractory tail buds showed very weak CoroNa Green signal (Fig. 3*C1*, white circle). In contrast, monensin-treated tails, after a 1 h current induction in high-sodium medium, showed a strong CoroNa Green fluorescence at the amputation site (Fig. 3*C2*, white circle), demonstrating that monensin treatment does increase intracellular sodium content in the regeneration bud.

We then assessed the consequence of monensin treatment on regeneration. During the refractory period, the regenerative ability of *Xenopus* tadpoles was extremely poor (RI = 16.8, $n = 179$). Most animals failed to regenerate any tissue in the amputated tails (Fig. 3*C3*). Strikingly, treatment at 18 hpa with 20 μM monensin in a medium containing 90 mM sodium for just 1 h induced a significant increase in both the quality and quantity of regeneration (RI = 48.5, $n = 101$, $p < 0.001$) compared with refractory controls (Fig. 3*C4*,*D*). The animals were developmentally normal and did not grow ectopic tissues. Importantly, the same treatment with either monensin alone (RI = 10.8, $n = 117$) or high extracellular sodium alone (RI = 20.8, $n = 125$) did not improve regenerative ability ($p > 0.05$), showing that neither monensin nor high extracellular sodium alone is capable of this effect and ruling out effects of osmolarity changes as an important factor in this treatment. It is the induced sodium influx that promotes regeneration. Consistent with our hypothesis, the same monensin induction method was observed to rescue another nonregenerative condition, caused by a pharmacological block of apoptosis (supplemental Fig. S3, available at www.jneurosci.org as supplemental material). Thus, the sufficiency of a transient pulse of sodium current at 18 hpa to restore regeneration demonstrates that control of the intracellular sodium level in the regeneration bud can be used as a brief treatment to initiate regeneration of a vertebrate neuromuscular appendage. This observation suggests that, surprisingly, this instructive signal does not have to be present at the time of injury and is not required long-term to drive regeneration.

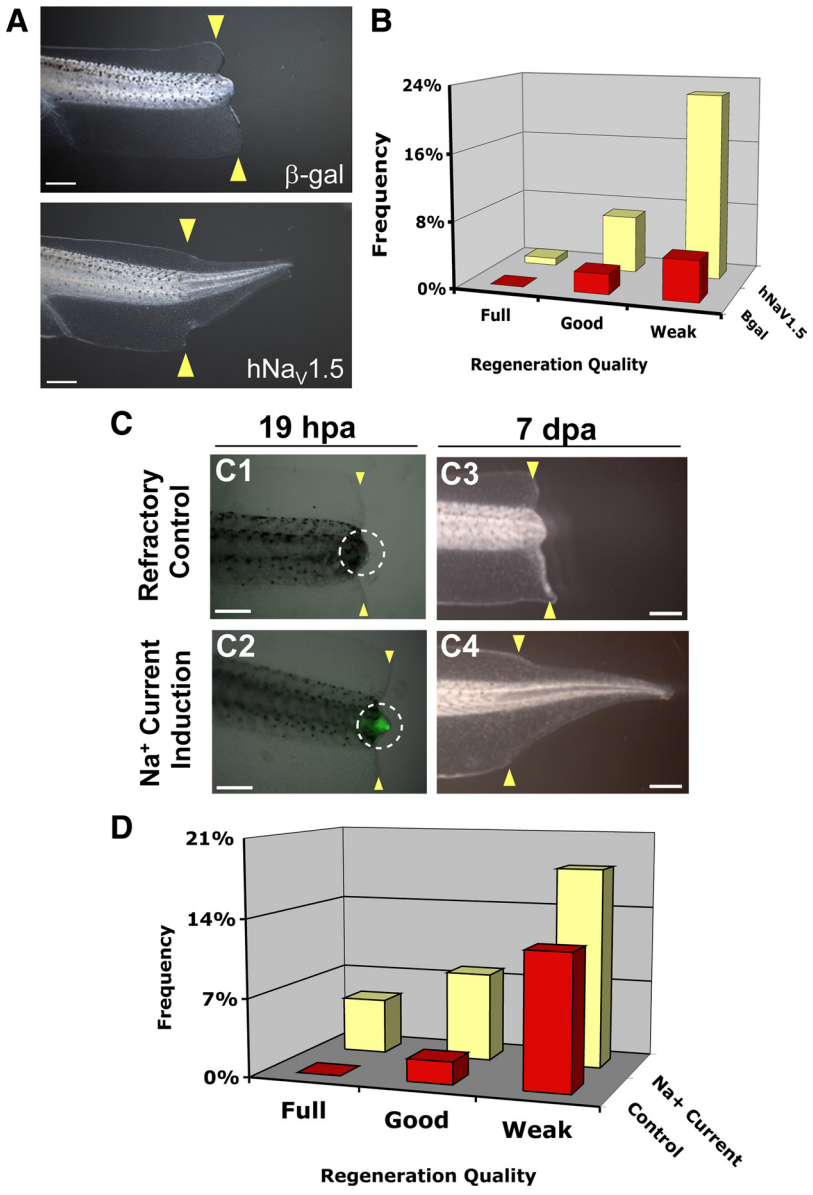

Figure 3. Transient induction of sodium current drives regeneration. ***A***, Regeneration rescue by human $Na_V1.5$ (h $Na_V1.5$). Control tail stumps (β-gal-injected) cut during the refractory period regenerate poorly, which is rescued by $hNa_V1.5$ expression. ***B***, Effects of regeneration rescue by $hNa_V1.5$ during refractory period block. ***C***, CoroNa Green analysis of sodium-current induction. ***C1***, Control (vehicle only), noninduced refractory stage bud has little CoroNa Green signal. ***C2***, Induction with 90 mM sodium and 20 μM monensin for 1 h (18–19 hpa) significantly increases intracellular sodium (green). Images are merged brightfield and fluorescence of the same exposure time. White circle, Refractory bud. ***C3***, Most refractory stage amputations fail to regenerate. ***C4***, Stimulation with sodium current restores full regeneration. ***D***, Transient sodium current rescues nonregenerative wound epidermis. Stimulation of sodium current increased regeneration more than twofold and improved regeneration quality compared with control siblings (treated with vehicle only, 0.01% ethanol). Treatment with either monensin or 90 mM sodium alone showed no effect. Scale bars: ***A***, 1 mm; ***C***, 500 μm.

Regenerative control through modulation of intracellular sodium levels

To gain a detailed mechanistic understanding of Na_V activity, we examined the consequences of modulating sodium ion transport

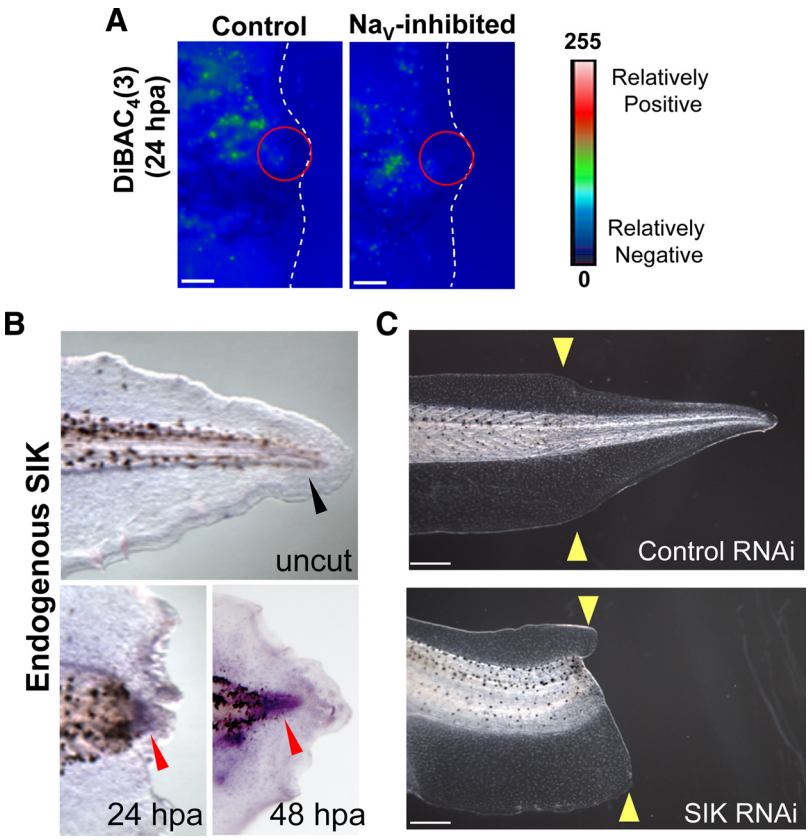

Figure 4. Salt-inducible kinase is required for tail regeneration. ***A***, Comparison of the relative voltage patterns of tail regeneration buds at 24 hpa using the voltage dye, DiBAC$_4$(3). Green is more depolarized than blue. Distal tail end (amputation site) is outlined in white. Scale bar, 100 μm. The regeneration bud (red circle) of controls was polarized (blue color). MS-222-treated buds show a similar pattern. ***B***, RNA *in situ* hybridization for endogenous SIK in whole-mount cut tails. SIK is expressed in the regeneration bud at 24 and 48 hpa (red arrows) but not in uncut tails (black arrow). ***C***, Effect of SIK RNAi on regeneration. SIK RNAi-expressing tadpoles fail to regenerate but develop normally.

in the regenerating tail. Na$_V$ activity is also a well known major determinant of some cells' membrane potential (V_{mem}), thus sodium flux could regulate regeneration by modulating the membrane voltage state of the regeneration bud. Using DiBAC4(3), we did not observe any changes in membrane voltage in the regeneration bud cells of MS-222-treated tails compared with controls (Fig. 4*A*, red circle), suggesting that, rather than changes in transmembrane potential, it is the sodium ion concentration *per se* that is the mechanism by which Na$_V$ function controls regenerative behavior.

One known effector of sodium ion-based signaling is the salt-inducible kinase (SIK), a member of the AMP-activated protein kinase family that responds to changes in intracellular sodium levels (Sanz, 2003). Because SIK is a potential candidate to act as a molecular sensor of Na$_V$ activity during regeneration, we searched for and were able to identify a single *Xenopus* SIK clone from a regeneration bud-specific cDNA library, which a BLAST search showed is most homologous to the SIK2 isoform. X-SIK is expressed in the regeneration bud at 24 and 48 hpa but not in the uncut tail (Fig. 4*B*). We found that when a SIK RNAi construct was expressed in the tail, overall development was normal but regeneration was significantly reduced compared with control dsRed RNAi (control, RI = 234; SIK, RI = 151; $n = 207$, $p < 0.001$) (Fig. 4*C*), demonstrating that SIK is indeed required for this process. Furthermore, pharmacological inhibition of SIK using staurosporine (STS) after sodium current induction during the refractory period also successfully blocked regeneration (no STS, RI = 54.4; 10 nM STS, RI = 1.8; $n = 225$, $p < 0.001$). Together, these results suggest that, as occurs in rats (Stenström et al., 2009), *Xenopus* SIK may transduce physiological sodium transport activity into second messenger cascades that control important cell functions necessary for tail regeneration, highlighting an important role for SIK during regeneration.

Discussion

Voltage-gated sodium channels have mainly been studied for their role in mediating the conduction of rapid electrical signaling in excitable cells of the nervous system and muscle (Diss et al., 2005), although roles in directing cell migration are beginning to be dissected (Brackenbury et al., 2008). The importance of bioelectric cues in regenerative events has been suggested for a very long time (Mathews, 1903; Lund, 1947). Both classical and recent work has indicated a requirement for sodium and electric fields in natural vertebrate appendage regeneration (Borgens et al., 1979; Robinson, 1983; Reid et al., 2009). However, the molecular source of regeneration-relevant currents in nonexcitable cells and the cell–biological consequences of their modulation remain largely unknown. Here we reveal a novel and unexpected role for Na$_V$-mediated sodium transport regulation of regeneration in a complex vertebrate structure. We show that sodium transport is required during the initiating stage of tail regeneration in *Xenopus*. Na$_V$1.2, but not Na$_V$1.5, is specifically expressed during endogenous regeneration and its expression is a predictor of regenerative ability—although additional unidentified Na$_V$s may also play a role in this process. It should be kept in mind that, although our quantitative analyses clearly indicate the efficacy of loss- and gain-of-function approaches targeting Na$_V$1.2, the penetrance of the inhibition and rescue had to be artificially suppressed by titering the treatments to low levels. This was made necessary by the importance of Na$_V$1.2 channels in the nervous system and heart; thus, overly strong modulation of sodium currents results in toxicity that would have made regeneration phenotypes impossible to detect. Along these lines, for example, our experiments with the Na$_V$1.2 blocker MS-222 were conducted at low levels that did not impair nerve function (i.e., did not cause paralysis or change in behavior).

Our results reveal both the upstream molecular pathways responsible for Na$_V$1.2-dependent induction of sodium flow (V-ATPase activity) (supplemental Fig. S2, available at www.jneurosci.org as supplemental material) and those downstream events controlled by sodium influx (Notch and Msx1 induction). The data characterized the effects of functional inhibition of sodium transport at several levels: physiologically (decrease of sodium influx), molecularly (lack of induction of regeneration-specific late genes, an effect likely mediated by SIK), and cellularly (changes in cell proliferation and axonal patterning). Together, these data suggest a model (Fig. 5) that integrates the biochemical, genetic, and

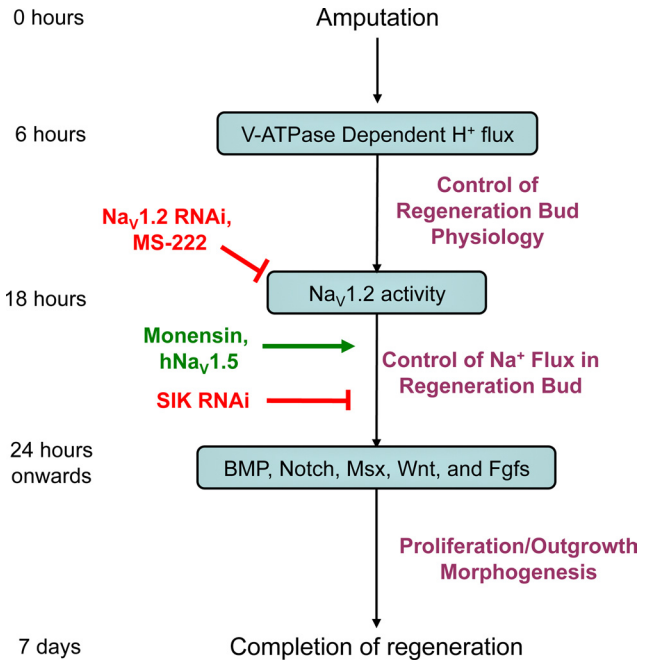

Figure 5. A model integrating Na_V in regeneration. By 6 hpa, the H^+ pump V-ATPase is expressed in the regeneration bud where it regulates the membrane voltage of the bud. V-ATPase activation results in the upregulation of $Na_V1.2$ by 18 hpa. Ablation of $Na_V1.2$ expression (RNAi) or Na_V function (pharmacological treatment) inhibits regeneration. Na_V activity enables sodium ions to enter regeneration bud cells and, potentially through SIK, to activate downstream pathways (such as BMP and Notch) by 24 hpa, driving regenerative outgrowth and patterning. By 7 d after injury, the rebuilding of the tail is largely complete. Importantly, monensin-mediated induction of a transient sodium flux into nonregenerative buds is sufficient to restore full tail regeneration, demonstrating that intracellular sodium signaling is a key regulator of regeneration able to initiate repair even after a nonregenerative wound epithelium has formed.

physiological data into a stepwise pathway leading to regeneration of the tail. Importantly, our model shows that the bioelectric signals produced by V-ATPase and Na_V form a physiological module; this module is both induced by and, in turn, influences gene expression while participating in the orchestration of multiple aspects of epimorphic regeneration.

A mechanism by which Na_V might be expected to function is through the control of membrane voltage. We found no evidence of this (Fig. 4), suggesting that regeneration bud cells regulate other transport events to maintain voltage despite changing levels of sodium ions. Furthermore, the results of the monensin experiments show that direct sodium increases are functionally instructive for regeneration during nonregenerative states that occur naturally (refractory period) (Fig. 3) or are induced chemically (apoptosis inhibition) (supplemental Fig. S3, available at www.jneurosci.org as supplemental material). These currents are endogenously provided by Na_V (and in *Xenopus* by $Na_V1.2$) but can be strikingly recapitulated by a very rapid, transient external induction of sodium flux. Although extracellular sodium currents are known to be a major component of transepithelial potentials (TEP) during repair in both *Xenopus* (Rajnicek et al., 1988; Jenkins et al., 1996) and humans (Shapiro et al., 2005), the mechanism we identified is different because it does not rely on modulation of the TEP. Our data most clearly support a role for intracellular sodium ions intrinsically guiding regenerative outgrowth through cell proliferation and gene expression in the bud—a novel mechanism for regeneration.

How then, does sodium flow control downstream events? Unlike calcium, relatively few effectors of sodium influx have been identified. Chemical treatments using inhibitors of either the sodium-activated potassium channel, Slo2.2 (Slo Inibitor treatment, RI = 270, $n = 74$; compared with control, RI = 258, $n = 33$; $p > 0.05$) or sodium/calcium exchangers (Adams et al., 2007) did not affect tail regeneration, suggesting that the effect of sodium is unlikely to be mediated by secondary effects on calcium. A likely candidate for transducing changes of intracellular sodium level into second messenger cascades is SIK, which has been implicated in stress response (Wang et al., 2008), global regulation of gene expression (Verdin et al., 2003), and may potentially regulate regenerative pathway genes such as BMPs (Shakèd et al., 2008). The identification of an increase of intracellular sodium as a key regulator of regenerative response is a crucial new area for future work integrating the roles of bioelectric signaling and the more canonical biochemical pathways (Blackiston et al., 2009; McCaig et al., 2009).

Na_V regulates regenerative growth in part by its influence on downstream signaling genes, including Notch1, BMP, and Msx1. These genes are also important for regeneration in other systems such as the tadpole limb, zebrafish fin and heart, and mammalian digit tips (Poss et al., 2000; Han et al., 2003). Consistent with the conserved roles of ion currents in regulating global patterning and morphogenetic cues from fungi to mammals (Nuccitelli et al., 1986; Levin, 2009), it is likely that the early mechanisms of ion transporter signaling in regeneration are used in other species and structures, in addition to the tail.

We show that several nonregenerative states (e.g., age-dependent decline or refractory period, and an apoptosis-inhibited failure of regeneration) can be rescued by a 1 h pharmacological treatment that recapitulates the Na_V-dependent influx of sodium in caudal bud cells and restores regeneration. Remarkably, this treatment only induced tail structures and did not generate ectopic growths or neoplasia during development, suggesting that sodium flow could act as a master control point to initiate tightly coordinated, self-limiting, downstream morphogenetic cascades (supplemental Fig. S4, available at www.jneurosci.org as supplemental material). This result has several important implications for regenerative medicine. The ability to restore regeneration using a temporally controllable pharmacological approach not requiring gene therapy is extremely exciting. Moreover, that a short-term induction of sodium current was sufficient to restore regeneration suggests the possibility that the correct initiating signal is not required long-term to drive completion of the process—a highly desirable property for regenerative therapies.

Most importantly, our finding that the amputated refractory tail can be induced to regenerate as late as 18 h after amputation reveals that tissues normally fated for regenerative failure still maintain their intrinsic ability and can be reprogrammed to reactivate regeneration. Furthermore, this observation challenges the view that differences in wound healing decisively determine regenerative ability (Tassava and Olsen, 1982; Campbell and Crews, 2008). In *Xenopus* tail regeneration, regenerative wound healing is completed by 8 hpa (Ho and Whitman, 2008). In contrast, refractory tail amputation results in a thickened, nonregenerative wound epidermis (Beck et al., 2003), which can be observed by 18 hpa (supplemental Fig. S5, available at www.jneurosci.org as supplemental material). Thus, the induction of a regenerative signal at 18 hpa is not predicted to impact wound healing. Our results demonstrate that nonregenerative wound healing is not a permanent block to the later induction of regeneration. That the instructive capacity of the wound epithelium can be overcome by biophysical signals such as that mediated by

Na_V reveals the existence of a competency window within which cells retain their capability to initiate the regenerative program—if the appropriate signals are provided. It also suggests that potential therapeutic treatments need not be administered immediately after acute injury (or indeed before injury, as is done in many studies of regenerative induction in this system). Further studies of the Na_V-mediated sodium transport regenerative signaling pathway will provide a detailed understanding of the requirements for initiating regeneration during different nonregenerative conditions and a more complete understanding of the molecular physiology of regeneration. Capitalizing upon such bioelectrical cues will be a rewarding and exciting area for regenerative medicine and developmental biology.

References

Adams DS, Masi A, Levin M (2006) *Xenopus* tadpole tail regeneration requires the activity of the proton pump V-ATPase, and proton pumping is sufficient to partially rescue the loss of function phenotype. Dev Biol 295:355–356.

Adams DS, Masi A, Levin M (2007) H+ pump-dependent changes in membrane voltage are an early mechanism necessary and sufficient to induce *Xenopus* tail regeneration. Development 134:1323–1335.

Armisén R, Fuentes R, Olguín P, Cabrejos ME, Kukuljan M (2002) Repressor element-1 silencing transcription/neuron-restrictive silencer factor is required for neural sodium channel expression during development of *Xenopus*. J Neurosci 22:8347–8351.

Beck CW, Christen B, Slack JM (2003) Molecular pathways needed for regeneration of spinal cord and muscle in a vertebrate. Dev Cell 5:429–439.

Beck CW, Christen B, Barker D, Slack JM (2006) Temporal requirement for bone morphogenetic proteins in regeneration of the tail and limb of *Xenopus* tadpoles. Mech Dev 123:674–688.

Beck CW, Izpisúa Belmonte JC, Christen B (2009) Beyond early development: *Xenopus* as an emerging model for the study of regenerative mechanisms. Dev Dyn 238:1226–1248.

Blackiston DJ, McLaughlin KA, Levin M (2009) Bioelectric controls of cell proliferation: ion channels, membrane voltage and the cell cycle. Cell Cycle 8:3519–3528.

Borgens RB, Vanable JW Jr, Jaffe LF (1979) Reduction of sodium dependent stump currents disturbs urodele limb regeneration. J Exp Zool 209:377–386.

Brackenbury WJ, Djamgoz MB, Isom LL (2008) An emerging role for voltage-gated Na+ channels in cellular migration: regulation of central nervous system development and potentiation of invasive cancers. Neuroscientist 14:571–583.

Campbell LJ, Crews CM (2008) Wound epidermis formation and function in urodele amphibian limb regeneration. Cell Mol Life Sci 65:73–79.

Chen Y, Lin G, Slack JM (2006) Control of muscle regeneration in the *Xenopus* tadpole tail by Pax7. Development 133:2303–2313.

Chera S, Ghila L, Dobretz K, Wenger Y, Bauer C, Buzgariu W, Martinou JC, Galliot B (2009) Apoptotic cells provide an unexpected source of Wnt3 signaling to drive hydra head regeneration. Dev Cell 17:279–289.

Coffman C, Harris W, Kintner C (1990) Xotch, the *Xenopus* homolog of *Drosophila* notch. Science 249:1438–1441.

Diss JK, Stewart D, Pani F, Foster CS, Walker MM, Patel A, Djamgoz MB (2005) A potential novel marker for human prostate cancer: voltage-gated sodium channel expression in vivo. Prostate Cancer Prostatic Dis 8:266–273.

Feledy JA, Beanan MJ, Sandoval JJ, Goodrich JS, Lim JH, Matsuo-Takasaki M, Sato SM, Sargent TD (1999) Inhibitory patterning of the anterior neural plate in *Xenopus* by homeodomain factors Dlx3 and Msx1. Dev Biol 212:455–464.

Fraser SP, Diss JK, Chioni AM, Mycielska ME, Pan H, Yamaci RF, Pani F, Siwy Z, Krasowska M, Grzywna Z, Brackenbury WJ, Theodorou D, Koyutürk M, Kaya H, Battaloglu E, De Bella MT, Slade MJ, Tolhurst R, Palmieri C, Jiang J, et al. (2005) Voltage-gated sodium channel expression and potentiation of human breast cancer metastasis. Clin Cancer Res 11:5381–5389.

Frazier DT, Narahashi T (1975) Tricaine (MS-222): effects on ionic conductances of squid axon membranes. Eur J Pharmacol 33:313–317.

Gargioli C, Slack JM (2004) Cell lineage tracing during *Xenopus* tail regeneration. Development 131:2669–2679.

Han M, Yang X, Farrington JE, Muneoka K (2003) Digit regeneration is regulated by Msx1 and BMP4 in fetal mice. Development 130:5123–5132.

Harland RM (1991) In situ hybridization: an improved whole mount method for *Xenopus* embryos. In: *Xenopus laevis*: practical uses in cell and molecular biology (Kay BK, Peng HB, eds), pp 685–695. San Diego: Academic.

Hedrick MS, Winmill RE (2003) Excitatory and inhibitory effects of tricaine (MS-222) on fictive breathing in isolated bullfrog brain stem. Am J Physiol Regul Integr Comp Physiol 284:R405–R412.

Ho DM, Whitman M (2008) TGF-beta signaling is required for multiple processes during *Xenopus* tail regeneration. Dev Biol 315:203–216.

Illingworth CM (1974) Trapped fingers and amputated finger tips in children. J Pediatr Surg 9:853–858.

Jenkins LS, Duerstock BS, Borgens RB (1996) Reduction of the current of injury leaving the amputation inhibits limb regeneration in the red spotted newt. Dev Biol 178:251–262.

Levin M (2004) A novel immunohistochemical method for evaluation of antibody specificity and detection of labile targets in biological tissue. J Biochem Biophys Methods 58:85–96.

Levin M (2009) Errors of geometry: regeneration in a broader perspective. Semin Cell Dev Biol 20:643–645.

Li F, Huang Q, Chen J, Peng Y, Roop DR, Bedford JS, Li CY (2010) Apoptotic cells activate the "phoenix rising" pathway to promote wound healing and tissue regeneration. Sci Signal 3:ra13.

Lund E (1947) Bioelectric fields and growth. Austin: University of Texas.

Mathews AP (1903) Electrical polarity in the hydroids. Am J Physiol 8:294–299.

McCaig CD, Song B, Rajnicek AM (2009) Electrical dimensions in cell science. J Cell Sci 122:4267–4276.

Meier SD, Kovalchuk Y, Rose CR (2006) Properties of the new fluorescent Na+ indicator CoroNa Green: comparison with SBFI and confocal Na+ imaging. J Neurosci Methods 155:251–259.

Miskevich F, Doench JG, Townsend MT, Sharp PA, Constantine-Paton M (2006) RNA interference of *Xenopus* NMDAR NR1 in vitro and in vivo. J Neurosci Methods 152:65–73.

Mochii M, Taniguchi Y, Shikata I (2007) Tail regeneration in the *Xenopus* tadpole. Dev Growth Differ 49:155–161.

Mollenhauer HH, Morré DJ, Rowe LD (1990) Alteration of intracellular traffic by monensin; mechanism, specificity and relationship to toxicity. Biochim Biophys Acta 1031:225–246.

Nieuwkoop PD, Faber J (1967) Normal table of *Xenopus laevis* (Daudin), 2nd Edition. Amsterdam: North-Holland Publishing Company.

Nuccitelli R, Robinson K, Jaffe L (1986) On electrical currents in development. Bioessays 5:292–294.

Poss KD, Shen J, Nechiporuk A, McMahon G, Thisse B, Thisse C, Keating MT (2000) Roles for Fgf signaling during zebrafish fin regeneration. Dev Biol 222:347–358.

Rajnicek AM, Stump RF, Robinson KR (1988) An endogenous sodium current may mediate wound healing in *Xenopus neurulae*. Dev Biol 128:290–299.

Reid B, Song B, McCaig CD, Zhao M (2005) Wound healing in rat cornea: the role of electric currents. FASEB J 19:379–386.

Reid B, Song B, Zhao M (2009) Electric currents in *Xenopus* tadpole tail regeneration. Dev Biol 335:198–207.

Robinson KR (1983) Endogenous electrical current leaves the limb and prelimb region of the *Xenopus* embryo. Dev Biol 97:203–211.

Saka Y, Smith JC (2001) Spatial and temporal patterns of cell division during early *Xenopus* embryogenesis. Dev Biol 229:307–318.

Sanz P (2003) Snf1 protein kinase: a key player in the response to cellular stress in yeast. Biochem Soc Trans 31:178–181.

Shakèd M, Weissmüller K, Svoboda H, Hortschansky P, Nishino N, Wölfl S, Tucker KL (2008) Histone deacetylases control neurogenesis in embryonic brain by inhibition of BMP2/4 signaling. PLoS One 3:e2668.

Shapiro S, Borgens R, Pascuzzi R, Roos K, Groff M, Purvines S, Rodgers RB, Hagy S, Nelson P (2005) Oscillating field stimulation for complete spinal cord injury in humans: a phase 1 trial. J Neurosurg Spine 2:3–10.

Singer M (1952) The influence of the nerve in regeneration of the amphibian extremity. Q Rev Biol 27:169–200.

Singer M (1965) A theory of the trophic nervous control of amphibian limb regeneration, including a re-evaluation of quantiative nerve requirements. In: Proceedings of regeneration in animals.

Sive HL, Grainger RM, Harland RM (2000) Early development of *Xenopus Laevis*. New York: Cold Spring Harbor Laboratory.

Slack JM, Beck CW, Gargioli C, Christen B (2004) Cellular and molecular mechanisms of regeneration in *Xenopus*. Philos Trans R Soc Lond B Biol Sci 359:745–751.

Stenström K, Takemori H, Bianchi G, Katz AI, Bertorello AM (2009) Blocking the salt-inducible kinase 1 network prevents the increases in cell sodium transport caused by a hypertension-linked mutation in human alpha-adducin. J Hypertens 27:2452–2457.

Sugiura T, Taniguchi Y, Tazaki A, Ueno N, Watanabe K, Mochii M (2004) Differential gene expression between the embryonic tail bud and regenerating larval tail in *Xenopus laevis*. Dev Growth Differ 46: 97–105.

Tassava RA, Olsen CL (1982) Higher vertebrates do not regenerate digits and legs because the wound epidermis is not functional. Differentiation 22:151–155.

Tseng AS, Adams DS, Qiu D, Koustubhan P, Levin M (2007) Apoptosis is required during early stages of tail regeneration in *Xenopus laevis*. Dev Biol 301:62–69.

Verdin E, Dequiedt F, Kasler HG (2003) Class II histone deacetylases: versatile regulators. Trends Genet 19:286–293.

Wang B, Goode J, Best J, Meltzer J, Schilman PE, Chen J, Garza D, Thomas JB, Montminy M (2008) The insulin-regulated CREB coactivator TORC promotes stress resistance in *Drosophila*. Cell Metab 7:434–444.

Yu FH, Catterall WA (2003) Overview of the voltage-gated sodium channel family. Genome Biol 4:207.

Zhao M, Song B, Pu J, Wada T, Reid B, Tai G, Wang F, Guo A, Walczysko P, Gu Y, Sasaki T, Suzuki A, Forrester JV, Bourne HR, Devreotes PN, McCaig CD, Penninger JM (2006) Electrical signals control wound healing through phosphatidylinositol-3-OH kinase-gamma and PTEN. Nature 442:457–460.

Zupanc GK (2006) Neurogenesis and neuronal regeneration in the adult fish brain. J Comp Physiol A Neuroethol Sens Neural Behav Physiol 192:649–670.

Communicative & Integrative Biology 6:1, e22595; January/February 2013; © 2013 Landes Bioscience

Cracking the bioelectric code

Probing endogenous ionic controls of pattern formation

AiSun Tseng[†] and Michael Levin*

Department of Biology and Tufts Center for Regenerative and Developmental Biology; Medford, MA USA

[†]Current affiliation: School of Life Sciences; University of Nevada-Las Vegas; Las Vegas, NV USA

Patterns of resting potential in non-excitable cells of living tissue are now known to be instructive signals for pattern formation during embryogenesis, regeneration and cancer suppression. The development of molecular-level techniques for tracking ion flows and functionally manipulating the activity of ion channels and pumps has begun to reveal the mechanisms by which voltage gradients regulate cell behaviors and the assembly of complex large-scale structures. A recent paper demonstrated that a specific voltage range is necessary for demarcation of eye fields in the frog embryo. Remarkably, artificially setting other somatic cells to the eye-specific voltage range resulted in formation of eyes in aberrant locations, including tissues that are not in the normal anterior ectoderm lineage: eyes could be formed in the gut, on the tail, or in the lateral plate mesoderm. These data challenge the existing models of eye fate restriction and tissue competence maps, and suggest the presence of a bioelectric code—a mapping of physiological properties to anatomical outcomes. This Addendum summarizes the current state of knowledge in developmental bioelectricity, proposes three possible interpretations of the bioelectric code that functionally maps physiological states to anatomical outcomes, and highlights the biggest open questions in this field. We also suggest a speculative hypothesis at the intersection of cognitive science and developmental biology: that bioelectrical signaling among non-excitable cells coupled by gap junctions simulates neural network-like dynamics, and underlies the information processing functions required by complex pattern formation in vivo. Understanding and learning to control the information stored in physiological networks will have transformative implications for developmental biology, regenerative medicine and synthetic bioengineering.

Keywords: bioelectricity, ion channels, pattern formation, regeneration

Submitted: 08/17/12

Accepted: 10/19/12

http://dx.doi.org/10.4161/cib.22595

*Correspondence to: Michael Levin;
Email: michael.levin@tufts.edu

Addendum to: Tseng AS, Beane WS, Lemire JM, Masi A, Levin M. Induction of vertebrate regeneration by a transient sodium current. J Neurosci 2010; 30:13192–200; PMID: 20881138; DOI: 10.1523/JNEUROSCI.3315-10.2010.

Introduction to Bioelectricity

It has long been known that all cells, not just excitable nerve and muscle, drive and respond to slow changes in transmembrane potential (V_{mem}).[1,2] Ion channels and pumps segregates charges to opposite sides of plasma and organelle membranes, producing slowly-changing differences in resting potential among cells in vivo (**Fig. 1**). Indeed spatial gradients of V_{mem} distributions exist also at the level of tissues and organs,[3] and have been long-known to correlate with important events in pattern formation such as gastrulation, neurogenesis and limb induction.[4-7] The classical data on developmental roles of endogenous bioelectric signals have recently been revitalized by the development of molecular-resolution genetic and pharmacological tools for the investigation and functional control of ionic signals in vivo.[8-10] Changes in resting potential regulate differentiation, proliferation, migration and orientation[11-13] of a wide variety of cell types, including stem cells, neurons and neuronal precursors and migratory populations such as neural crest. Recent data have implicated spatiotemporal patterns of V_{mem} in the regulation of embryonic development, regeneration and

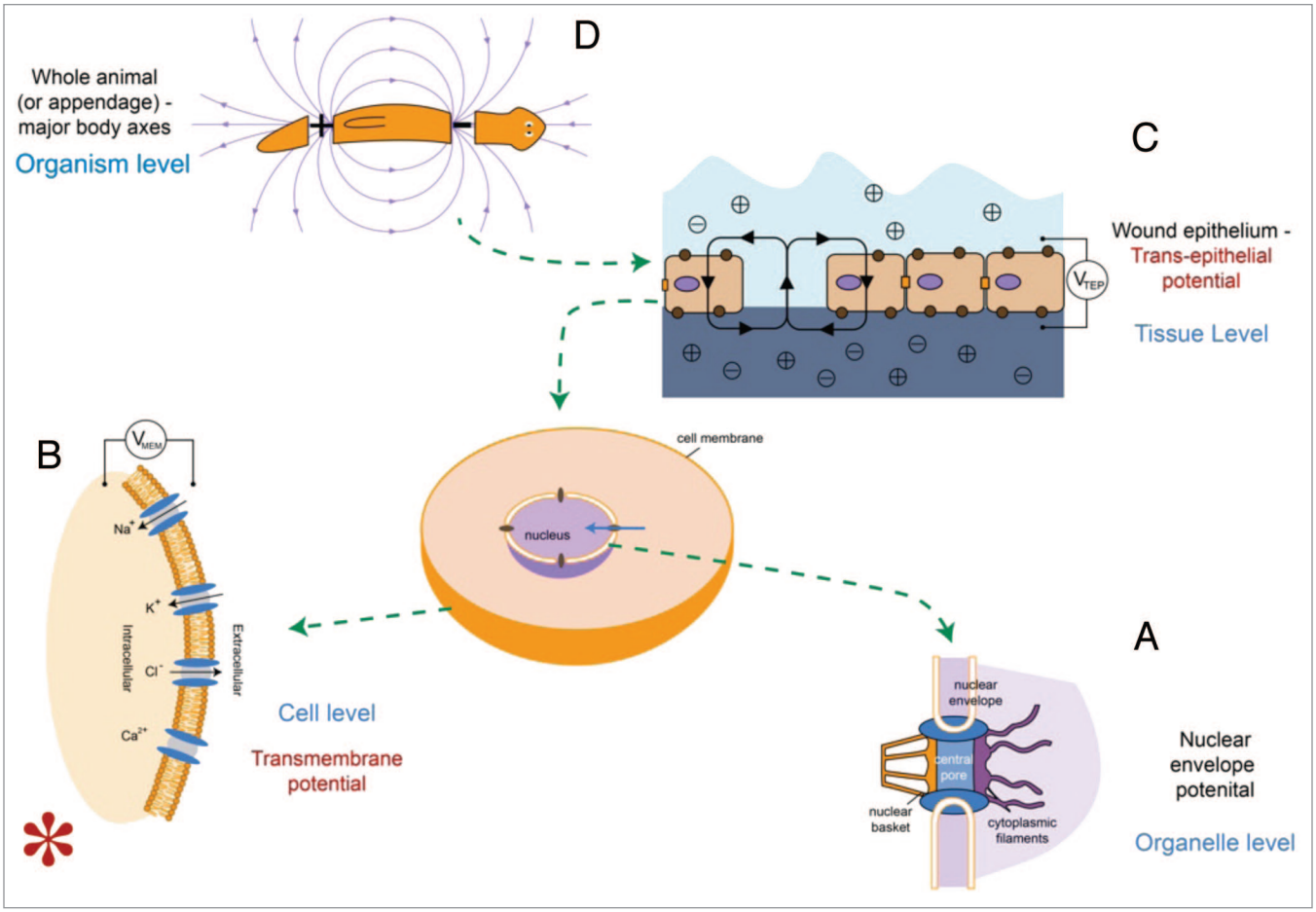

Figure 1. Multi-scale bioelectric gradients in vivo. Segregation of ions by ion channel and pump proteins, and open high-conductivity paths (through gap junctions, cytoplasm and extracellular fluids), produce gradients of voltage potential. These exist at the level of organelles (e.g., nuclear envelope potential, **A**), cells (transmembrane potential, **B**), tissues (transepithelial potential, **C**) and even whole animal axes or appendages (**D**). Schematic drawn by Maria Lobikin.

metastatic transformation.[14] Thus, bioelectric cues function alongside chemical gradients, transcriptional networks, and haptic/tensile cues as part of the morphogenetic field that orchestrates individual cell behavior into large-scale anatomical pattern formation.[15,16]

Recent work in tractable model systems has shown that bioelectric cues serve as mediators of positional information[17] and determinants of anatomical identity during growth and morphostasis.[18,19] Endogenous bioelectric fields mediate wound healing by coordinating epithelial closure,[20] initiate complex appendage regeneration,[21,22] regulate neoplastic transformation,[23,24] determining the left-right asymmetry of internal organs,[25,26] control differentiation of mammalian adult[27] and embryonic[28] stem cells, and even dictate the large-scale anatomy (producing head vs. tail) of tissues derived from the blastema in regenerating flatworms.[18] Importantly, these coherent changes of anatomy have been analyzed to reveal the mechanistic steps leading from voltage change to cell behavior,[10,29] revealing regulation of small signaling molecules' movement through transporters as a common scheme for transducing bioelectrical changes into transcriptional[23,30,31] and epigenetic[29,32,33] readouts.

Importantly, in a number of cases, it has been shown that the patterning change produced by a specific bioelectric signal (e.g., eye induction, neoplastic transformation, left-right asymmetry generation) is dependent only on the voltage itself, not on the genetic identity of the channel or the chemical species of the ion involved; in most cases, the same downstream effects on cells' behavior are induced by a given V_{mem} state regardless of whether that state was achieved by movement of potassium, sodium, or chloride ions,[19,23,26,30,34] or of which ion translocators' activity resulted in the given potential change. Because the V_{mem} of cells can be set by post-translational gating of ion channels, pumps and gap junctions (not just at the level of gene expression), this is a true epigenetic layer of control (in Waddington's original sense of the word.) The instructive signal is often borne by the physiological state itself, not the genetic identity of any particular ion channel or pump gene.

Thus, patterning information at the level of physiology regulates morphogenesis in a number of systems. In parallel with the genetic and epigenetic codes, this implies the existence of a bioelectric

code—a quantitative mapping between ionic properties of cellular structures and anatomical outcome. Further progress necessitates a synthesis—a conceptual understanding of how biophysical properties of cells may be interpreted by growing tissues into specific changes of growth and form. Interestingly, recent data suggest three different ways by which biological structures decode bioelectric patterns.

Eye Induction by Control of V_{mem}

The development of voltage-sensitive fluorescent dyes has facilitated the non-invasive tracking of ionic gradients within single cells (**Fig. 2A**) and during complex pattern formation (**Fig. 2B**).[35,36] Moreover, strategies for targeted misexpression of well-characterized ion translocator proteins allow the investigator to specifically depolarize or hyperpolarize select cell groups in vivo during loss- or gain-of-function experiments.[37] These techniques recently converged to shed new light on a paradigm case of embryonic pattern formation: eye development in the frog *Xenopus* laevis.[19]

A survey of spatiotemporal distributions of V_{mem} during craniofacial development[35] revealed two spots of hyperpolarized cells that become eyes; artificial depolarization of these cells by misexpression of a cation channel altered expression of endogenous eye markers and induced eye defects. Conversely, misexpression of a number of channels could drive non-eye-field cells into the resting potential range associated with eye induction (**Fig. 2C**), initiating a feedback loop between hyperpolarization and Pax6 expression, and causing the formation of complete eyes (**Fig. 2D**). Most excitingly, this could occur far outside the anterior neural field (where exogenous Pax6 alone cannot initiate eye formation): eyes could be formed in the gut, tail, or lateral plate mesoderm! These data significantly extend our understanding of lineage restrictions and competence during development; a specific range of resting potential was able to drive cells well outside of the anterior neurectoderm into an eye fate and form complete organs. What are the implications of these data in the wider context of the field of bioelectricity and molecular developmental biology?

Major Open Questions About the Bioelectric Code

For any code, it is crucial to ask what outcomes are mapped onto which observable properties of the coding medium. For example, the well-established genetic code maps the structure of DNA into the sequence of protein building blocks, but it does not directly specify morphology. Precisely what aspects of pattern are encoded by biophysical properties of cells? Three major (non-mutually-exclusive) possibilities have been suggested by the latest data.

The first is that of spatiotemporal gradients of V_{mem} within cells and tissues as direct prepattern for growth and form, an idea that was first proposed decades ago.[38,39] Recent studies of bioelectric changes in the developing amphibian face[35] reveal that iso-electric domains of voltage regionalize the growing tissue-bioelectric properties distributed across ell fields directly form a template controlling gene expression much as patterns of gene expression (e.g., HOX code) underlie the anatomy of vertebra, limbs and whole embryos. According to this hypothesis, the way to understand bioelectric influences is at the level of control of gene expression domains in tissue, and that this code can be capitalized upon by imposing desired patterns upon tissue by manipulation of the V_{mem} (e.g., repairing birth defects by inducing the right pattern of voltage gradients within tissue primordial that thus correct the expression patterns of key downstream patterning genes). We are currently developing optogenetic[40] strategies that would allow the real-time rewriting of bioelectric patterns in vivo.

A second possible function of the bioelectric code is a mapping of voltage ranges to specific anatomical structures. For example, a narrow range of transmembrane potential is necessary and sufficient for demarcating the eye field (**Fig. 2C and D**) while depolarized or hyperpolarized V_{mem} determines whether a head or tail forms at a wound blastema in planaria (**Fig. 2E and F**). On this model, there may be specific voltage ranges corresponding to individual organs, such as eyes, heads, or hearts (**Fig. 3A and B**); indeed, given the fact that each cell has not one but many domains of different V_{mem} along its surface (**Fig. 2A**), the spatial distribution of voltage values could form an even richer combinatorial code and store a significant amount of information for a cell as well as its neighbors. Thus, it is imperative to discover whether additional voltage ranges are associated with the formation of various organ structures, and if so, whether the quantitative nature of this mapping is the same across different model systems and across individuals of the same species. Note that this view focuses on one organizational level higher than the prepattern model, since here the functional association of specific V_{mem} values is with an entire complex organ, not with direct control of transcriptional patterns within cell fields.

Interestingly, recent data demonstrated the existence of an even higher-level effect. In the tadpole tail, during the refractory period at which the tail normally does not regenerate (**Fig. 3C and E**), induction of proton pumping or sodium influx can kick-start the regeneration of an entire appendage including spinal cord, muscle, vasculature and peripheral innervation. In both cases, very little information was provided by the initiating bioelectrical signal, as we did not modulate the ion flux in any way. These findings were most intriguing since following amputation, we could induce the regrowth of an appendage without knowing, or having to specify, the detailed structure of the organ (a finding with obvious implications for regenerative biomedicine). Instead of micromanaging its assembly (a task beyond today's bioengineering capabilities), the appropriate bioelectric signal is apparently able to activate the host's coherent, self-limiting morphogenetic subroutine corresponding to tail formation. Note that unlike the ectopic eyes and posterior heads (**Fig. 2**), in this case the appropriate structure (heart or tail) is formed at the appropriate location (**Fig. 3**) without our matching the signal to any specific property of these structures. Thus, we wondered whether in some cases, the bioelectric signal also activates a positional information pathway

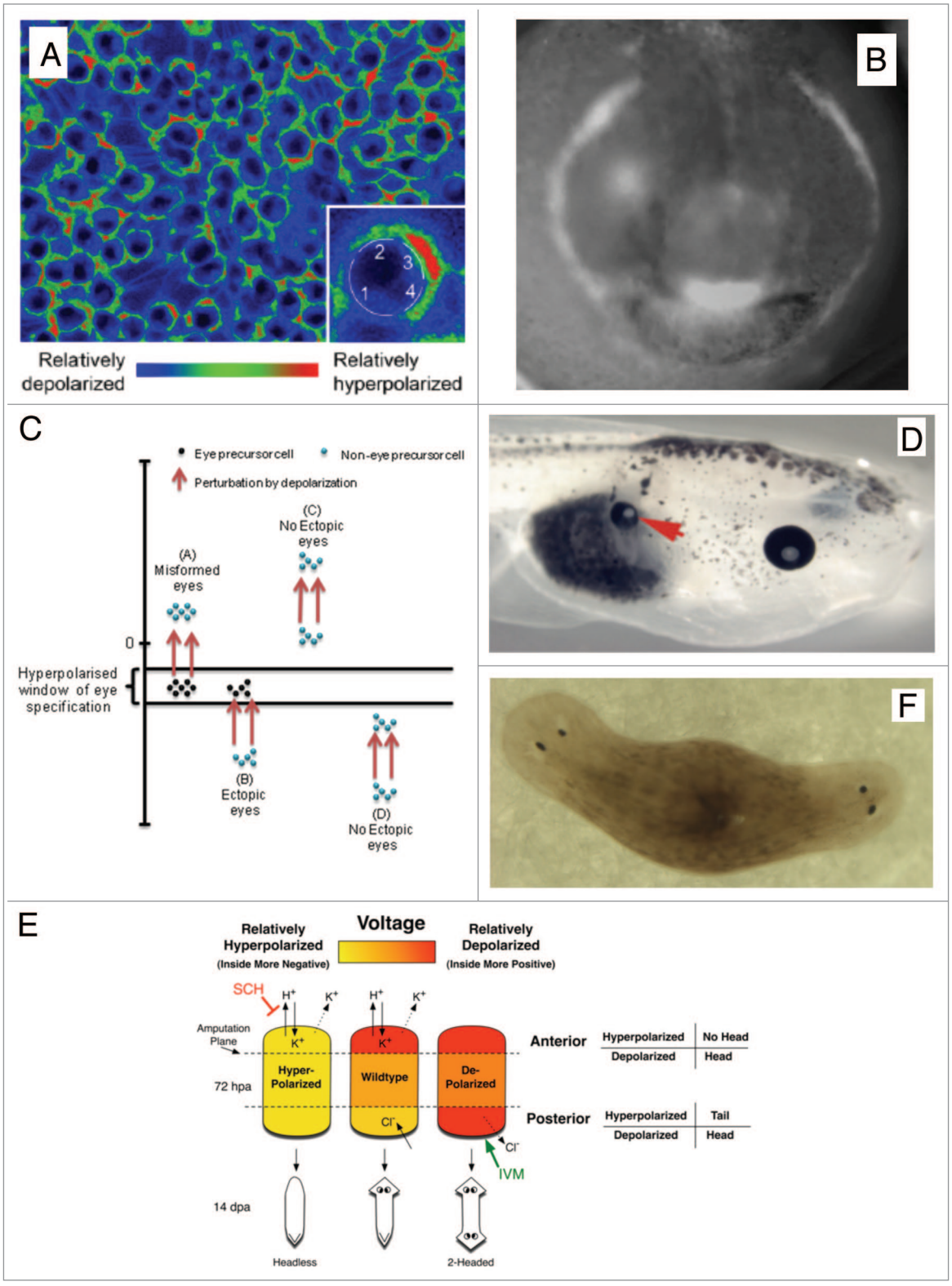

Figure 2. Bioelectric properties regulate large-scale morphology. (**A**) Voltage-sensitive dyes reveal domains within membranes of individual cells in culture—each cell contains not one but a manifold of transmembrane voltage values.[37] (**B**) At the level of organogenesis, patterns of hyperpolarized cells (lighter stain) drive craniofacial patterning in *Xenopus* laevis. These patterns determine gene expression domains (e.g., *Frizzled*) and are instructive for morphogenesis of the face.[35] Artificially setting the resting potential in embryonic frog cells in vivo to a narrow range that corresponds to eye fate (**C**) forces cell groups far outside the anterior neural field (e.g., gut or mesoderm cells) to form complete eyes (**D**).[19] Beyond single organs, manipulation of V_{mem} in accordance with a predictive model (**E**) allows rational control of large-scale pattern produced by the activity of adult stem cells in planaria; panel **F** shows a 2-headed worm in which a pharmacological technique was used to reset posterior blastema identity to that of a head by inducing the bioelectrical polarization value that determines anterior tissue fate.

that guides the induced growth toward the locally-appropriate anatomical identity.

To test this hypothesis, we used the same cocktail that induced tail regeneration (**Fig. 2E and F**) on a tadpole hindlimb amputation. We found (**Fig. 4**) no instances of a tail or any other non-limb structure forming at the wound site; instead, a number of (normally non-regenerative) animals grew back hindlimbs, including the most distal components (toes and even toe-nails); these limbs were sensitive to touch and motile (see Video S1). This remarkable effect is not only promising with respect to biomedical use of this technology to induce repair and regeneration of complex structures, but also reveals that the same biophysical signal can induce different (appropriate) structures at distinct anatomical locations.

Conclusion and Hypothesis: What's Next for Molecular Bioelectricity?

The field of bioelectricity is at an extremely exciting juncture. Molecular-level tools now exist, and a number of recent papers have demonstrated the importance of these physiological signals and shown how they interface to canonical biochemical/genetic pathways.[9,10,13] These data have taught us a number of important lessons. First, that resting potential is not simply a basic parameter needed for cell health. Much as information is routinely encoded in a subtle modulatory signal coexisting with a strong carrier wave in radio-communications, it is possible to experimentally dissociate the bioelectricity needed for housekeeping processes from the developmental roles of voltage patterns. Second, experimental modulation of voltage in vivo is a powerful method for making large-scale, coherent changes in anatomy. Thus, patterns of ionic properties among non-excitable cells are endogenous instructive parameters that not only control basic behaviors of individual cells, but also serve as regulators of shape at the organ and whole organism level. As such, these pathways are a tractable and attractive control point for biomedical strategies in the areas of birth defects, regeneration and cancer suppression.

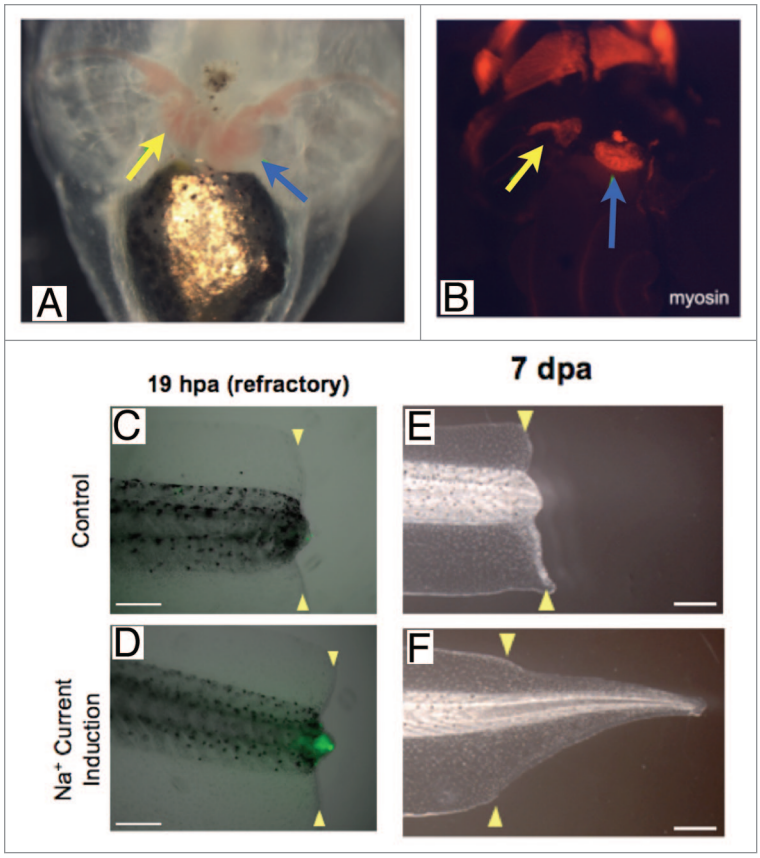

Figure 3. Bioelectric signals produce appropriate organs at appropriate locations. (**A and B**) Misexpression of specific ion channels (unpublished data, obtained by Sherry S. Aw) induces beating, ectopic hearts (indicated by yellow arrows) to be formed next to the original (primary heart, indicated by blue arrows). Likewise, at a stage when tails no longer regenerate in tadpoles (**C and E**) simple induction of a 1 h sodium flux into the tail (**D**) causes regeneration (**E**) of the entire tail.[21] In both cases, the information content of the bioelectric event is very low—a simple signal can kickstart a complex, downstream morphogenetic cascade appropriate to the location within the host.

The next steps in this field[41] must involve expanded efforts to obtain comprehensive physiomic profiling data that can be mined for quantitative analysis of the bioelectric code. Since many different ion channels can contribute to the same V_{mem}, and many different V_{mem} levels can arise from the post-translational gating of exactly the same set of channels and pumps, proteomic or transcriptome analysis inevitably miss information inherent in bioelectric properties. The profiling data, using combinations of electrodes and reporter dyes, must be merged with functional analyses using state-of-the-art methods for manipulating V_{mem} in vivo. One of the most exciting future lines of research concerns the development of chemical strategies for conferring light sensitivity to native ion channels,[42,43] allowing optical control of ion flux with heretofore unprecedented spatiotemporal resolution. As these pathways become better understood, bioelectric elements will be encapsulated as modules that can be plugged into existing bioengineering frameworks, adding greatly to the power of the current set of building blocks in synthetic biology.[44,45]

Looking further ahead beyond the immediate biomedical and engineering applications of bioelectricity, fully unlocking the promise of bioelectricity will require a novel conceptual apparatus with which to understand and learnt to exploit the dynamics of information encoded in the real-time dynamics of physiological (electrical) networks among tissues (**Fig. 5A**). Bioinformatics and modeling tools must be developed

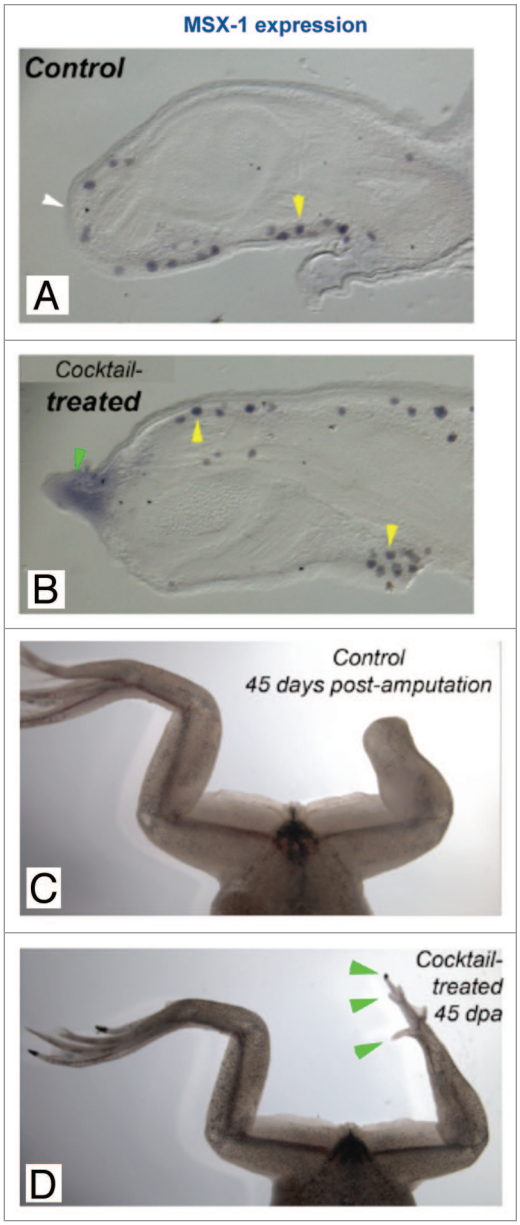

Figure 4. Na^+ induction promotes limb regeneration. To determine whether the sodium influx that triggered tail regeneration was specific for tail identity or triggered events that interacted with positional information cues (initiated a spatially-appropriate response), we tested the same monensin cocktail that initiated tail regeneration on a tadpole leg amputation model. Hind limbs of st. 57 tadpoles were amputated at the tibia-fibula location. At 1 dpa, tapoles were treated either with 0.1% Ethanol (Control) or with a cocktail of 20uM Monensin and 90mM Na-Gluconate in 0.1XMMR for 1 h. Tadpoles were allowed to recover and grown at 23C until froglet stage. Sectioning during early stages revealed that compared with control limbs (**A**), cocktail-treated limbs upregulated MSX-1, a regenerative marker at the wound edge [green arrowhead, compare with lack of MSX-1-positive region in (**A**) indicated by white arrowhead (**B**)]. Yellow arrowheads indicate additional cells expressing MSX-1 away from the wound (present in all limbs, treated or controls). Within 45 d, compared with very little or no (**C**) growth in controls, relatively improved regrowth at the amputation site was seen in the treated animals (**D**). These regenerated hindlimbs often included toes and toenails (green arrowheads), indicative of proper distal morphogenesis. Notably, in no cases (n = 28) were non-limb structures observed.

that truly capture the unique signaling properties of physiological networks and merge them with the current crop of techniques that focus on gene-regulatory networks in multi-scale models of complex biological systems. The existing models of cardiac and brain physiology are not directly suitable because they focus on action potentials and spiking dynamics, rather than the very different propagation and slow changes of resting potential that occur in non-excitable tissues.

However, we speculate that the tools of cognitive neuroscience can be extended to understand the electrical communication among non-neuronal cells. During regeneration and embryogenesis, organs frequently determine their size, ascertain their shape relative to a target morphology, recognize specific stimuli, exhibit habituation and sensitization to signals, and make decisions based on current information and data stored from prior events. We now know that many of these processes are under control of bioelectrical mechanisms. Is it possible that the ability of organs and tissues to remodel and dynamically maintain/restore specific 3-dimensional shape is a result of computations they perform via electric signaling[46]? The cognitive properties of neural networks, and the success of information processing technologies (e.g., computer science) strongly suggest that bioelectrical communication is a universal and convenient medium by which to control complex events like pattern formation. Although this remains to be tested, such a hypothesis is highly compatible with evolutionary conservation of fundamental mechanisms and the increasingly-observed parallels between developmental mechanisms and neural information processing.[47]

As is beginning to be appreciated for astrocyte and glial networks,[48,49] and has been suggested for bone[50] and even plant cells,[51] many different interconnected cell types could be functionally isomorphic with neural networks (**Fig. 5B**). Resting V_{mem} levels are analogous to the "node activation" of neural net models, while voltage-sensitive, often asymmetric gap junctions mediating cell:cell links can readily play the role of synapses. Thus, our hypothesis is that the existing highly successful theoretical apparatus for information processing in neurobiology could be extended to understand the properties of highly dynamic, self-repairing tissues and organs.[15,52] We are embarking on a

research program to determine whether quantitative, predictive models of information storage and exchange can be used to explain the cognitive-like functions of morphogenetic systems. This is an interdisciplinary effort that blurs the line between the mechanisms of spatial information (shape, target morphology) and those of temporal information (pattern in time-dependent signals, learning and memory). We hypothesize that the rich and deep techniques of computational neuroscience can be applied to understand and manipulate the functions of dynamically remodeling tissues. If true, such unification would result in truly transformative advances in synthetic morphology, bioengineering, hybrid cybernetic biorobotics and regenerative medicine.

Disclosure of Potential Conflicts of Interest

No potential conflicts of interest were disclosed.

Acknowledgments

We thank Anne Rajnicek, Colin McCaig and other members of the bioelectricity community, Daniel C. Dennett, and the Levin Lab for many useful discussions. This work is supported by National Institutes of Health (EY018168, AR061988, GM078484, AR055993), the G. Harold and Leila Y. Mathers Charitable Foundation and the Telemedicine and Advanced Technology Research Center at the US Army Medical Research and Materiel Command through awardW81XWH-10–2-0058.

Supplemental Material

Supplemental material may be found here: www.landesbioscience.com/journals/cib/article/22595

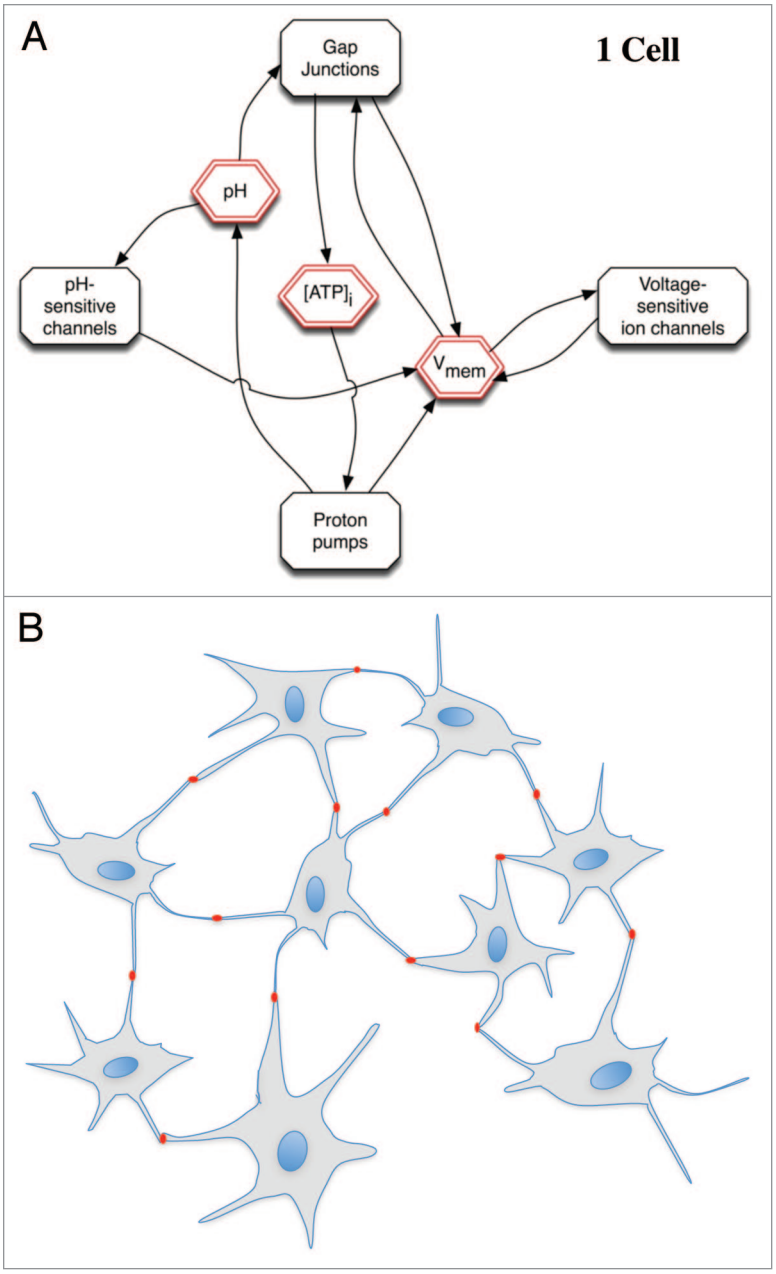

Figure 5. Physiological networks can store information. (**A**) At the level of a single cell, ion translocator proteins are both regulated by, and regulate, voltage. The network of physiological parameters and post-translational states of ion channels and pumps implements rich feedback loops, which can support multistable attractor states and thus store information in the resting potential state of cells.[53] (**B**) Collections of cells coupled by gap junctions implement neural-like networks, since the voltage-sensitive gap junctions play the role of synapses, and each cell has the ability to occupy multiple V_{mem} states based on electrical signals from its neighbors. It is thus very likely that computational tissues could be made from non-excitable cells.

References

1. Lund E. Bioelectric fields and growth. Austin: Univ. of Texas Press, 1947.
2. Levin M, Stevenson CG. Regulation of cell behavior and tissue patterning by bioelectrical signals: challenges and opportunities for biomedical engineering. Annu Rev Biomed Eng 2012; 14:295-323; PMID:22809139; http://dx.doi.org/10.1146/annurev-bioeng-071811-150114.
3. Robinson K, Messerli M. Electric embryos: the embryonic epithelium as a generator of developmental information. In: McCaig C, ed. Nerve Growth and Guidance. Portland: Portland Press, 1996:131-41.
4. Nuccitelli R, Robinson K, Jaffe L. On electrical currents in development. Bioessays 1986; 5:292-4; PMID:2436612; http://dx.doi.org/10.1002/bies.950050616.
5. Nuccitelli R. Endogenous ionic currents and DC electric fields in multicellular animal tissues. Bioelectromagnetics 1992; (Suppl 1): 147-57; PMID:1285710; http://dx.doi.org/10.1002/bem.2250130714.
6. Robinson KR, Messerli MA. Left/right, up/down: the role of endogenous electrical fields as directional signals in development, repair and invasion. Bioessays 2003; 25:759-66; PMID:12879446; http://dx.doi.org/10.1002/bies.10307.
7. Jaffe LF. Control of development by ionic currents. In: Cone RA, and John E. Dowling, eds., ed. Membrane Transduction Mechanisms. New York: Raven Press, 1979.

8. Reid B, Zhao M. Ion-selective self-referencing probes for measuring specific ion flux. Commun Integr Biol 2011; 4:524-7; PMID:22046453.
9. Levin M. Bioelectric mechanisms in regeneration: Unique aspects and future perspectives. Semin Cell Dev Biol 2009; 20:543-56; PMID:19406249; http://dx.doi.org/10.1016/j.semcdb.2009.04.013.
10. Levin M. Large-scale biophysics: ion flows and regeneration. Trends Cell Biol 2007; 17:261-70; PMID:17498955; http://dx.doi.org/10.1016/j.tcb.2007.04.007.
11. Blackiston DJ, McLaughlin KA, Levin M. Bioelectric controls of cell proliferation: ion channels, membrane voltage and the cell cycle. Cell Cycle 2009; 8:3519-28; PMID:19823012; http://dx.doi.org/10.4161/cc.8.21.9888.
12. Yao L, McCaig CD, Zhao M. Electrical signals polarize neuronal organelles, direct neuron migration, and orient cell division. Hippocampus 2009; 19:855-68; PMID:19280605; http://dx.doi.org/10.1002/hipo.20569.
13. McCaig CD, Song B, Rajnicek AM. Electrical dimensions in cell science. J Cell Sci 2009; 122:4267-76; PMID:19923270; http://dx.doi.org/10.1242/jcs.023564.
14. Levin M. Molecular bioelectricity in developmental biology: new tools and recent discoveries: control of cell behavior and pattern formation by transmembrane potential gradients. Bioessays 2012; 34:205-17; PMID:22237730; http://dx.doi.org/10.1002/bies.201100136.
15. Levin M. Morphogenetic fields in embryogenesis, regeneration, and cancer: non-local control of complex patterning. Biosystems 2012; 109:243-61; PMID:22542702; http://dx.doi.org/10.1016/j.biosystems.2012.04.005.
16. Burr HS, Northrop FSC. The electro-dynamic theory of life. Q Rev Biol 1935; 10:322-33; http://dx.doi.org/10.1086/394488.
17. Shi R, Borgens RB. Three-dimensional gradients of voltage during development of the nervous system as invisible coordinates for the establishment of embryonic pattern. Dev Dyn 1995; 202:101-14; PMID:7734729; http://dx.doi.org/10.1002/aja.1002020202.
18. Beane WS, Morokuma J, Adams DS, Levin M. A chemical genetics approach reveals H,K-ATPase-mediated membrane voltage is required for planarian head regeneration. Chem Biol 2011; 18:77-89; PMID:21276941; http://dx.doi.org/10.1016/j.chembiol.2010.11.012.
19. Pai VP, Aw S, Shomrat T, Lemire JM, Levin M. Transmembrane voltage potential controls embryonic eye patterning in Xenopus laevis. Development 2012; 139:313-23; PMID:22159581; http://dx.doi.org/10.1242/dev.073759.
20. Zhao M, Song B, Pu J, Wada T, Reid B, Tai G, et al. Electrical signals control wound healing through phosphatidylinositol-3-OH kinase-gamma and PTEN. Nature 2006; 442:457-60; PMID:16871217; http://dx.doi.org/10.1038/nature04925.
21. Tseng AS, Beane WS, Lemire JM, Masi A, Levin M. Induction of vertebrate regeneration by a transient sodium current. J Neurosci 2010; 30:13192-200; PMID:20881138; http://dx.doi.org/10.1523/JNEUROSCI.3315-10.2010.
22. Adams DS, Masi A, Levin MH. H+ pump-dependent changes in membrane voltage are an early mechanism necessary and sufficient to induce Xenopus tail regeneration. Development 2007; 134:1323-35; PMID:17329365; http://dx.doi.org/10.1242/dev.02812.
23. Blackiston D, Adams DS, Lemire JM, Lobikin M, Levin M. Transmembrane potential of GlyCl-expressing instructor cells induces a neoplastic-like conversion of melanocytes via a serotonergic pathway. Dis Model Mech 2011; 4:67-85; PMID:20959630; http://dx.doi.org/10.1242/dmm.005561.
24. Morokuma J, Blackiston D, Adams DS, Seebohm G, Trimmer B, Levin M. Modulation of potassium channel function confers a hyperproliferative invasive phenotype on embryonic stem cells. Proc Natl Acad Sci USA 2008; 105:16608-13; PMID:18931301; http://dx.doi.org/10.1073/pnas.0808328105.
25. Levin M. Is the early left-right axis like a plant, a kidney, or a neuron? The integration of physiological signals in embryonic asymmetry. Birth Defects Res C Embryo Today 2006; 78:191-223; PMID:17061264; http://dx.doi.org/10.1002/bdrc.20078.
26. Levin M, Thorlin T, Robinson KR, Nogi T, Mercola M. Asymmetries in H+/K+-ATPase and cell membrane potentials comprise a very early step in left-right patterning. Cell 2002; 111:77-89; PMID:12372302; http://dx.doi.org/10.1016/S0092-8674(02)00939-X.
27. Sundelacruz S, Levin M, Kaplan DL. Membrane potential controls adipogenic and osteogenic differentiation of mesenchymal stem cells. PLoS ONE 2008; 3:e3737; PMID:19011685; http://dx.doi.org/10.1371/journal.pone.0003737.
28. Lange C, Prenninger S, Knuckles P, Taylor V, Levin M, Calegari F. The H(+) vacuolar ATPase maintains neural stem cells in the developing mouse cortex. Stem Cells Dev 2011; 20:843-50; PMID:21126173; http://dx.doi.org/10.1089/scd.2010.0484.
29. Tseng A-S, Levin M. Transducing bioelectric signals into epigenetic pathways during tadpole tail regeneration. Anat Rec 2012; In press; http://dx.doi.org/10.1002/ar.22495.
30. Adams DS, Robinson KR, Fukumoto T, Yuan S, Albertson RC, Yelick P, et al. Early, H+-V-ATPase-dependent proton flux is necessary for consistent left-right patterning of non-mammalian vertebrates. Development 2006; 133:1657-71; PMID:16554361; http://dx.doi.org/10.1242/dev.02341.
31. Fukumoto T, Kema IP, Levin M. Serotonin signaling is a very early step in patterning of the left-right axis in chick and frog embryos. Curr Biol 2005; 15:794-803; PMID:15886096; http://dx.doi.org/10.1016/j.cub.2005.03.044.
32. Tseng AS, Carneiro K, Lemire JM, Levin M. HDAC activity is required during Xenopus tail regeneration. PLoS ONE 2011; 6:e26382; PMID:22022609; http://dx.doi.org/10.1371/journal.pone.0026382.
33. Carneiro K, Donnet C, Rejtar T, Karger BL, Barisone GA, Díaz E, et al. Histone deacetylase activity is necessary for left-right patterning during vertebrate development. BMC Dev Biol 2011; 11:29; PMID:21599922; http://dx.doi.org/10.1186/1471-213X-11-29.
34. Aw S, Adams DS, Qiu D, Levin MH. H,K-ATPase protein localization and Kir4.1 function reveal concordance of three axes during early determination of left-right asymmetry. Mech Dev 2008; 125:353-72; PMID:18160269; http://dx.doi.org/10.1016/j.mod.2007.10.011.
35. Vandenberg LN, Morrie RD, Adams DS. V-ATPase-dependent ectodermal voltage and pH regionalization are required for craniofacial morphogenesis. Dev Dyn 2011; 240:1889-904; PMID:21761475; http://dx.doi.org/10.1002/dvdy.22685.
36. Adams DS, Levin M. General principles for measuring resting membrane potential and ion concentration using fluorescent bioelectricity reporters. Cold Spring Harb Protoc 2012; 2012:385-97; PMID:22474653; http://dx.doi.org/10.1101/pdb.top067710.
37. Adams DS, Levin M. Endogenous voltage gradients as mediators of cell-cell communication: strategies for investigating bioelectrical signals during pattern formation. Cell Tissue Res 2012; PMID:22350846; http://dx.doi.org/10.1007/s00441-012-1329-4.
38. Burr HS, Hovland CI. Bio-Electric Correlates of Development in Amblystoma. Yale J Biol Med 1937; 9:540-9; PMID:21433741.
39. Burr HS, Northrop FSC. Evidence for the Existence of an Electro-Dynamic Field in Living Organisms. Proc Natl Acad Sci USA 1939; 25:284-8; PMID:16577899; http://dx.doi.org/10.1073/pnas.25.6.284.
40. Fenno L, Yizhar O, Deisseroth K. The development and application of optogenetics. Annu Rev Neurosci 2011; 34:389-412; PMID:21692661; http://dx.doi.org/10.1146/annurev-neuro-061010-113817.
41. Levin M. The wisdom of the body: future techniques and approaches to morphogenetic fields in regenerative medicine, developmental biology and cancer. Regen Med 2011; 6:667-73; PMID:22050517; http://dx.doi.org/10.2217/rme.11.69.
42. Fortin DL, Dunn TW, Kramer RH. Engineering light-regulated ion channels. Cold Spring Harb Protoc 2011; 2011:579-85; PMID:21632787; http://dx.doi.org/10.1101/pdb.top112.
43. Fortin DL, Dunn TW, Fedorchak A, Allen D, Montpetit R, Banghart MR, et al. Optogenetic photochemical control of designer K+ channels in mammalian neurons. J Neurophysiol 2011; 106:488-96; PMID:21525363; http://dx.doi.org/10.1152/jn.00251.2011.
44. Regot S, Macia J, Conde N, Furukawa K, Kjellén J, Peeters T, et al. Distributed biological computation with multicellular engineered networks. Nature 2011; 469:207-11; PMID:21150900; http://dx.doi.org/10.1038/nature09679.
45. Bashor CJ, Horwitz AA, Peisajovich SG, Lim WA. Rewiring cells: synthetic biology as a tool to interrogate the organizational principles of living systems. Annu Rev Biophys 2010; 39:515-37; PMID:20192780; http://dx.doi.org/10.1146/annurev.biophys.050708.133652.
46. Hauser H, Ijspeert AJ, Füchslin RM, Pfeifer R, Maass W. Towards a theoretical foundation for morphological computation with compliant bodies. Biol Cybern 2012; PMID:22290137.
47. Boettiger A, Ermentrout B, Oster G. The neural origins of shell structure and pattern in aquatic mollusks. Proc Natl Acad Sci USA 2009; 106:6837-42; PMID:19351900; http://dx.doi.org/10.1073/pnas.0810311106.
48. Blomstrand F, Aberg ND, Eriksson PS, Hansson E, Rönnbäck L. Extent of intercellular calcium wave propagation is related to gap junction permeability and level of connexin-43 expression in astrocytes in primary cultures from four brain regions. Neuroscience 1999; 92:255-65; PMID:10392848; http://dx.doi.org/10.1016/S0306-4522(98)00738-6.
49. Pannasch U, Vargová L, Reingruber J, Ezan P, Holcman D, Giaume C, et al. Astroglial networks scale synaptic activity and plasticity. Proc Natl Acad Sci USA 2011; 108:8467-72; PMID:21536893; http://dx.doi.org/10.1073/pnas.1016650108.
50. Turner CH, Robling AG, Duncan RL, Burr DB. Do bone cells behave like a neuronal network? Calcif Tissue Int 2002; 70:435-42; PMID:12149636; http://dx.doi.org/10.1007/s00223-001-1024-z.
51. Volkov AG, Carrell H, Adesina T, Markin VS, Jovanov E. Plant electrical memory. Plant Signal Behav 2008; 3:490-2; PMID:19704496; http://dx.doi.org/10.4161/psb.3.7.5684.
52. Vandenberg LN, Adams DS, Levin M. Normalized shape and location of perturbed craniofacial structures in the Xenopus tadpole reveal an innate ability to achieve correct morphology. Dev Dyn 2012; 241:863-78; PMID:22411736; http://dx.doi.org/10.1002/dvdy.23770.
53. Gallaher J, Bier M, van Heukelom JS. First order phase transition and hysteresis in a cell's maintenance of the membrane potential--An essential role for the inward potassium rectifiers. Biosystems 2010; 101:149-55; PMID:20566338; http://dx.doi.org/10.1016/j.biosystems.2010.05.007.